

COLOUR-INDEPENDENT PARTITION FUNCTIONS IN COLOURED VERTEX MODELS

O FODA¹ AND M WHEELER²

ABSTRACT. We study lattice configurations related to \mathcal{S}_n , the scalar product of an off-shell state and an on-shell state in rational A_n integrable vertex models, $n \in \{1, 2\}$. The lattice lines are colourless and oriented. The state variables are n conserved colours that flow along the line orientations, but do not necessarily cover every bond in the lattice.

Choosing boundary conditions such that the positions where the colours flow into the lattice are fixed, and where they flow out are summed over, we show that the partition functions of these configurations, with these boundary conditions, are n -independent. Our results extend to trigonometric A_n models, and to all n .

This n -independence explains, in vertex-model terms, results from recent studies of \mathcal{S}_2 [1, 2]. Namely, **1.** \mathcal{S}_2 , which depends on two sets of Bethe roots, $\{b_1\}$ and $\{b_2\}$, and cannot (as far as we know) be expressed in single determinant form, degenerates in the limit $\{b_1\} \rightarrow \infty$, and/or $\{b_2\} \rightarrow \infty$, into a product of determinants, **2.** Each of the latter determinants is an A_1 vertex-model partition function.

1. INTRODUCTION AND MOTIVATION

The subject of this paper is integrable periodic spin chains and vertex models with rational and trigonometric A_n R -matrices $n \in \{1, 2, \dots\}$. We focus on the rational models, and on $n \in \{1, 2\}$, to simplify the presentation and the proofs but, as we will explain, our conclusions extend without modification to the trigonometric models, and to all n .

We wish to show that there are A_n -model partition functions that are independent of the number of colours n . In other words, if one considers a set of these A_n configurations, regards the n colours as identical, and re-evaluates the partition function as if these were A_1 configurations, the result would be the same.

1.1. Two types of Bethe states. There are two types of Bethe states in the space of states of an integrable A_n rational or trigonometric spin chain or vertex model [3, 4, 5]. **1.** Off-shell Bethe states $\{\alpha\}$ which are characterized by rapidity variables that are free, and are not eigenstates of the transfer matrix. **2.** On-shell Bethe states $\{\beta\}$ which are characterized by rapidity variables that satisfy Bethe equations, and are eigenstates of the transfer matrix.

1.2. Three types of scalar products. There are three types of scalar products between Bethe states. **1.** The off-shell/off-shell scalar product $\mathcal{K}_n(\alpha_i, \alpha_j) = \langle \alpha_i | \alpha_j \rangle$. A sum expression was obtained in [6] for \mathcal{K}_1 , and in [7] for \mathcal{K}_2 . \mathcal{K}_n cannot be expressed in single determinant form. **2.** The off-shell/on-shell scalar product $\mathcal{S}_n(\alpha_i, \beta_j) = \langle \alpha_i | \beta_j \rangle$. \mathcal{S}_1 was evaluated in determinant form in [8]. A second determinant expression was obtained in [9], and a third was obtained in [10]. **3.** The on-shell/on-shell scalar product $\mathcal{G}_n(\beta_i, \beta_j) = \langle \beta_i | \beta_j \rangle$, which vanishes for $i \neq j$, since the on-shell Bethe states are orthogonal [11, 3], and gives the (square of the) norm of $|\beta_i\rangle$, $\mathcal{G}_n(\beta_i, \beta_i) = \langle \beta_i | \beta_i \rangle$, for $i = j$. A determinant expression was obtained in [12, 11] for \mathcal{G}_1 , in [7] for \mathcal{G}_2 , and conjectured in [15] for all \mathcal{G}_n .

1.3. Structure constants of operators in A_1 scalar sub-sectors of SYM₄. Building on applications of integrability in supersymmetric Yang-Mills theories¹, the off-shell/off-shell scalar product \mathcal{K}_1 , as well as the norm \mathcal{G}_1 , were used in [15, 16] to compute the tree-level

Key words and phrases. A_n vertex models. Scalar products.

¹For a comprehensive overview of integrability in Yang-Mills theories with particular emphasis on the AdS/CFT correspondence, see [13]. For a more compact review, see [14].

structure constants $\mathcal{C}_{ijk}^{(0)}$ of 3-point functions of gauge-invariant local composite operators in the A_1 scalar sub-sectors of planar $\mathcal{N} = 4$ supersymmetric Yang-Mills theory, SYM₄. In these computations, all three operators involved correspond to non-BPS states. In [17], the semi-classical limit of $\mathcal{C}_{ijk}^{(0)}$ was computed in the case where two of the operators involved correspond to BPS states.

In [18], the off-shell/on-shell scalar product \mathcal{S}_1 , as well as the norm \mathcal{G}_1 , were used to express $\mathcal{C}_{ijk}^{(0)}$, with three non-BPS operators, in determinant form. The result of [18] was extended to A_1 sub-sectors in planar Yang-Mills theories with fewer supersymmetries in [19], as well as planar QCD in [20]. In [19], we further showed that $\mathcal{C}_{ijk}^{(0)}$ is a discrete KP τ -function in the free auxiliary rapidities that characterize an off-shell spin-chain state used to represent one of the operators in the 3-point function.

Determinant expressions are ideally suited to numerical evaluations as well as to computing the asymptotics of the quantities that they represent. In [21, 22], Kostov wrote the determinant expression of $\mathcal{C}_{ijk}^{(0)}$, with three non-BPS states, in terms of free fermions, and from that obtained its semi-classical limit.

In [24], Gromov and Vieira showed that given $\mathcal{C}_{ijk}^{(0)}$ in spin-chain terms and in the presence of inhomogeneous quantum rapidities, the 1-loop (and possibly 2-loop) corrections are obtained by applying a certain differential operator in the quantum rapidities. In [25], Serban discussed an extension of this statement to all loops. In [10], we showed that the 1-loop-corrected version of $\mathcal{C}_{ijk}^{(0)}$ of [24] can be put in determinant form.

1.4. Structure constants of operators in A_2 scalar sub-sectors of SYM₄. Following the developments in computing A_1 scalar sub-sector structure constants outlined above, it is natural to look for analogous results in the A_2 scalar sub-sectors as the next step towards evaluating SYM₄ structure constants in all generality. However, while there is a sum expression for \mathcal{K}_2 due to Reshetikhin [7], there is no determinant expression for \mathcal{S}_2 . Moreover, recent results suggest that no such determinant form exists [26, 27].

1.5. Degenerate A_2 scalar products and colour independence. There are determinant expressions for degenerations of \mathcal{S}_2 obtained by taking some or all of the Bethe roots to infinity [1, 2]. This is surprising, not only because these expressions are products of determinants, but also because each of these determinants is an A_1 vertex model partition function.

In combinatorial terms, one starts with \mathcal{S}_2 and regards that as a partition function of configurations in three state variables. Degenerating \mathcal{S}_2 by taking one set or both sets of Bethe roots to infinity, one obtains what can be thought of as the product of partition functions of configurations of two, rather than three state variables. If the initial state variables are $\{\textit{white}, \textit{black}, \textit{blue}\}$, the final state variables are $\{\textit{white}, \textit{black}\}$ and all dependence on the colour blue has disappeared.

1.6. Aim of this work. We wish to show that the results of [1, 2] follow from the fact that there are A_2 , or more generally A_n ($n = 2, 3, 4, \dots$) vertex-model lattice configurations whose partition functions are n -independent, and from that we show that **1**. The partition function corresponding to \mathcal{S}_2 factorizes, and **2**. The factors are A_1 expressions that can be evaluated in determinant form.

1.7. Outline of contents. In Section **2**, we recall the basics of rational and trigonometric A_n vertex models. In **3** and **4**, we recall the A_1 domain wall and scalar product configurations. In **5**, we introduce an extra colour in A_1 configurations, thereby turning them into A_2 configurations. This can be further extended to obtain A_n configurations. In **6** and **7** we study the ‘coloured’ version of the A_1 domain wall and scalar product, which are A_2 configurations. In **8**, we apply the results obtained in previous sections to A_2 scalar product configurations. Section **9** contains various remarks. An appendix contains various technical details.

2. THE A_n VERTEX MODEL

2.1. Rapidity variables, lattice lines and coloured state variables. A_n vertex model partition functions depend on up to $2n$ sets of auxiliary rapidities, and n sets of quantum rapidities. The auxiliary rapidities may satisfy Bethe equations, so they are ‘Bethe roots’, or they are free. The quantum rapidities, or ‘inhomogeneities’, are free. We work in the inhomogeneous setting where the quantum rapidities are not necessarily equal. We use $\{\alpha\}$ for the set of elements $\alpha_1, \alpha_2, \dots$, and denote its cardinality by $|\alpha|$.

All lattice lines are oriented, and the rapidities can be viewed as flowing along the lattice lines in the same direction as the line orientations. The state variables of the A_n model, ι , take values in the set $\{0, 1, \dots, n\}$. We shall think of the state variable assignments $\iota \in \{1, 2, \dots, n\}$ as *colours* that flow in the same directions as the rapidities along the line orientations, and of the assignment $\iota = 0$ as a colourless, or *white* background. Among the colours $\{1, 2, \dots, n\}$ we distinguish $\iota = 1$ as *black*. With this definition, A_1 model configurations consist of only black and white. $A_{n \geq 2}$ model configurations are genuinely coloured. The aim of this work is to show that certain coloured configurations in $A_{n \geq 2}$ models are equivalent to black and white ones in the A_1 model.

For $n = 1$, the auxiliary rapidities flow in horizontal lines from left to right and the quantum rapidities flow in vertical lines from bottom to top. For $n = 2, 3, \dots$, the rapidities flow in well-defined directions that are indicated on the diagrams.

We use $\{x^{(i)}\}$, $i \in \{1, \dots, n\}$, for the i -th set of auxiliary rapidities that are always free, and define $|x| = |x^{(1)}| + \dots + |x^{(n)}|$. We use $\{b^{(i)}\}$, $i \in \{1, \dots, n\}$, for the i -th set of auxiliary rapidities that are sometimes assumed to satisfy Bethe equations (depending on context), and define $|b| = |b^{(1)}| + \dots + |b^{(n)}|$. In fact the only time we require the $\{b^{(i)}\}$ to be Bethe roots is when we seek a determinant evaluation of a partition function that depends on them. The rest of the time they can be considered free. We use $\{y\}$ for the quantum rapidities, or inhomogeneities, so that $|y| = L$, where L is the length of the spin chain. Finally, we use the notation

$$(1) \quad \Delta\{x\}_N = \prod_{1 \leq i < j \leq N} (x_j - x_i), \quad \Delta\{-x\}_N = \prod_{1 \leq i < j \leq N} (x_i - x_j)$$

for the Vandermonde determinant in the set $\{x\} = \{x_1, \dots, x_N\}$.

2.2. R -matrices and vertex weights. We are interested in solutions of the Yang-Baxter equation

$$(2) \quad R_{\alpha\beta}(x, y)R_{\alpha\gamma}(x, z)R_{\beta\gamma}(y, z) = R_{\beta\gamma}(y, z)R_{\alpha\gamma}(x, z)R_{\alpha\beta}(x, y)$$

that are based on A_n algebras. These are $(n+1)^2 \times (n+1)^2$ R -matrices of the form

$$(3) \quad R_{\alpha\beta}^{(n)}(x, y) = a(x, y) \sum_{0 \leq i \leq n} E_{\alpha}^{(ii)} E_{\beta}^{(ii)} \\ + \sum_{0 \leq i < j \leq n} \left(b_+(x, y) E_{\alpha}^{(ii)} E_{\beta}^{(jj)} + b_-(x, y) E_{\alpha}^{(jj)} E_{\beta}^{(ii)} \right) \\ + \sum_{0 \leq i < j \leq n} \left(c_+(x, y) E_{\alpha}^{(ij)} E_{\beta}^{(ji)} + c_-(x, y) E_{\alpha}^{(ji)} E_{\beta}^{(ij)} \right)$$

where $E_{\alpha}^{(ij)}$ is an $(n+1) \times (n+1)$ elementary matrix acting on the vector space $V_{\alpha} = \mathbb{C}^{n+1}$, whose (i, j) -th entry is 1 while all remaining entries are 0. The functions a, b_{\pm}, c_{\pm} are defined to be

$$(4) \quad a(x, y) = 1, \quad b_{\pm}(x, y) = \frac{x - y}{x - y + 1}, \quad c_{\pm}(x, y) = \frac{1}{x - y + 1}$$

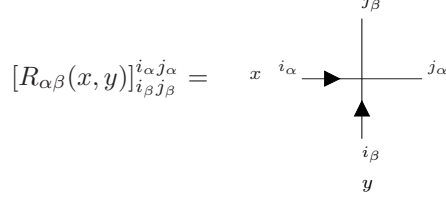


Figure 1: In $[R_{\alpha\beta}(x, y)]_{i_\beta j_\beta}^{i_\alpha j_\alpha}$, the (i_α, j_α) -th component of the R -matrix acts on V_α , and the (i_β, j_β) -th component of the R -matrix acts on V_β . We associate $[R_{\alpha\beta}(x, y)]_{i_\beta j_\beta}^{i_\alpha j_\alpha}$ with the vertex shown.

for rational models, and

$$(5) \quad a(x, y) = 1, \quad b_\pm(x, y) = e^{\mp\gamma} \frac{[x - y]}{[x - y + \gamma]}, \quad c_\pm(x, y) = e^{\pm(x-y)} \frac{[\gamma]}{[x - y + \gamma]}$$

for trigonometric models, where we use the notation $[x] = \sinh(x)$. The R -matrices (3) have $(n + 1)(2n + 1)$ non-zero entries, which can be identified with vertices according to the convention shown in Figure 1. We call the resulting $(n + 1)(2n + 1)$ -vertex model the A_n vertex model.

2.3. The R -matrix of the A_1 model. The simplest of the models discussed above, corresponding to the case $n = 1$, is the six-vertex model. Using the general formula (3), the A_1 R -matrix can be written as

$$(6) \quad R_{\alpha\beta}(x, y) = \begin{pmatrix} a(x, y) & 0 & 0 & 0 \\ 0 & b_+(x, y) & c_+(x, y) & 0 \\ 0 & c_-(x, y) & b_-(x, y) & 0 \\ 0 & 0 & 0 & a(x, y) \end{pmatrix}_{\alpha\beta}$$

and we match its entries with the vertices shown in Figure 2. In $A_{n \geq 2}$ models, we continue to refer to vertices as a , b or c vertices when they are of the form shown in Figure 2 but with 0 and/or 1 replaced by more general colours.

3. A_1 DOMAIN WALL PARTITION FUNCTION

3.1. Definition of the DWPF. The domain wall partition function is a function in two sets of variables $\{x\}_N = \{x_1, \dots, x_N\}$ and $\{y\}_N = \{y_1, \dots, y_N\}$, and we denote it by $Z(\{x\}_N | \{y\}_N)$. We define this quantity to be the partition function of the lattice shown in Figure 3.

3.2. Properties of the DWPF. Following [6], the rational DWPF satisfies a set of four properties which determine it uniquely.

A. $Z(\{x\}_N | \{y\}_N)$ is a meromorphic function of the form

$$(7) \quad Z(\{x\}_N | \{y\}_N) = \frac{P(\{x\}_N | \{y\}_N)}{\prod_{i,j=1}^N (x_i - y_j + 1)}$$

where $P(\{x\}_N | \{y\}_N)$ is a polynomial of degree $N - 1$ in the variable x_N .

B. $Z(\{x\}_N | \{y\}_N)$ is symmetric in the set of variables $\{y_1, \dots, y_N\}$.

C. By setting $x_N = y_N$, we obtain the recursion relation

$$(8) \quad Z(\{x\}_N | \{y\}_N) \Big|_{x_N=y_N} = Z(\{x\}_{N-1} | \{y\}_{N-1})$$

D. In the case $N = 1$, we have $Z(x_1 | y_1) = c_-(x_1, y_1)$.

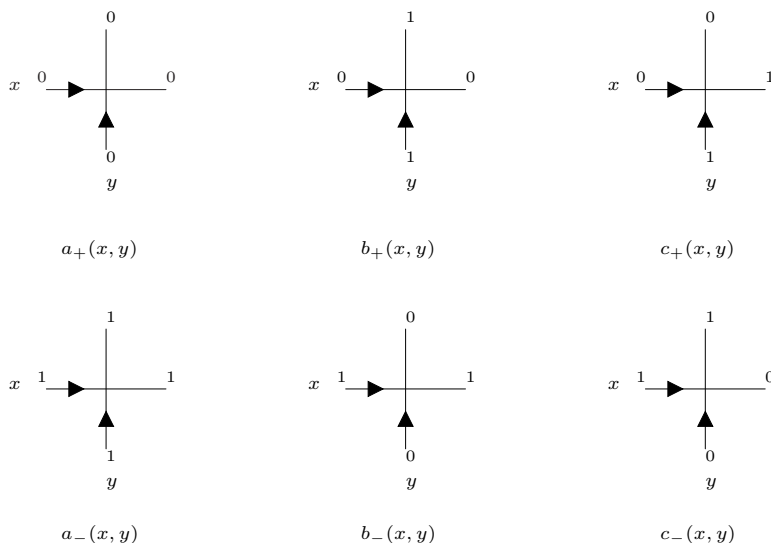


Figure 2: Identifying the entries of the R -matrix with vertices. For the purpose of making each vertex weight unique, we have defined $a_+(x, y) = a_-(x, y) = a(x, y)$.

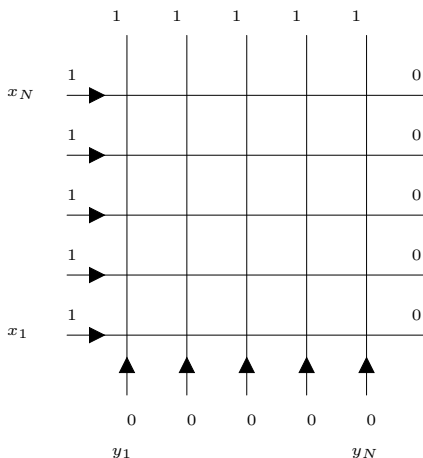


Figure 3: Lattice representation of $Z(\{x\}_N | \{y\}_N)$. Every intersection of a horizontal and vertical line is a vertex, as defined in Figure 2. The colours on all external segments are fixed to the values shown, while all internal segments are summed over.

Proof. We prove these properties using the lattice representation of the DWPF in Figure 3.

A. We assume that the factor $\frac{1}{(x_i - y_j + 1)^2}$ is common to any weight at the intersection of the i -th horizontal and j -th vertical lines², so the denominator in (7) is explained. For the numerator, it is easy to see that the top line of the lattice in Figure 3 (which contributes all x_N dependence to the DWPF) must contain exactly one c_- vertex, which has degree 0 in x_N . This explains the fact that $P(\{x\}_N | \{y\}_N)$ is degree $N - 1$ in x_N .

B. The symmetry in $\{y_1, \dots, y_N\}$ is proved using the following argument for interchanging two vertical lattice lines. Consider multiplying the DWPF by the a vertex $a(y_{j+1}, y_j) \equiv 1$.

²By writing $a(x_i, y_j) = \frac{(x_i - y_j + 1)}{(x_i - y_j + 1)}$.

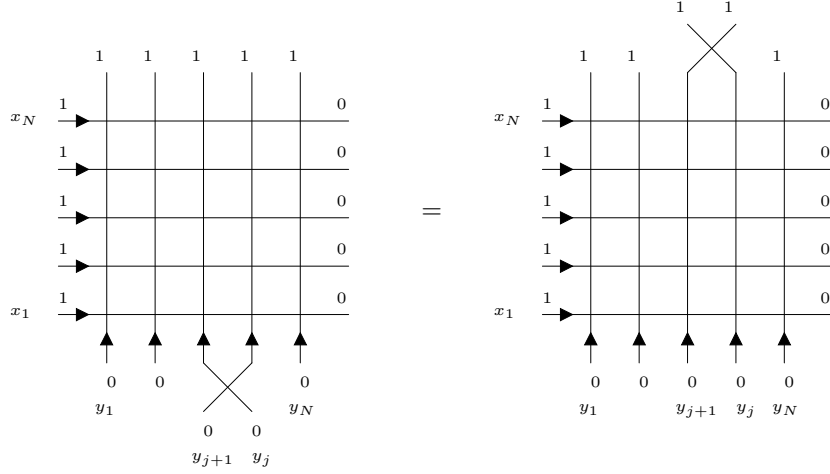


Figure 4: Interchanging two vertical lattice lines. The inserted vertex is translated vertically through the lattice using the Yang-Baxter equation.

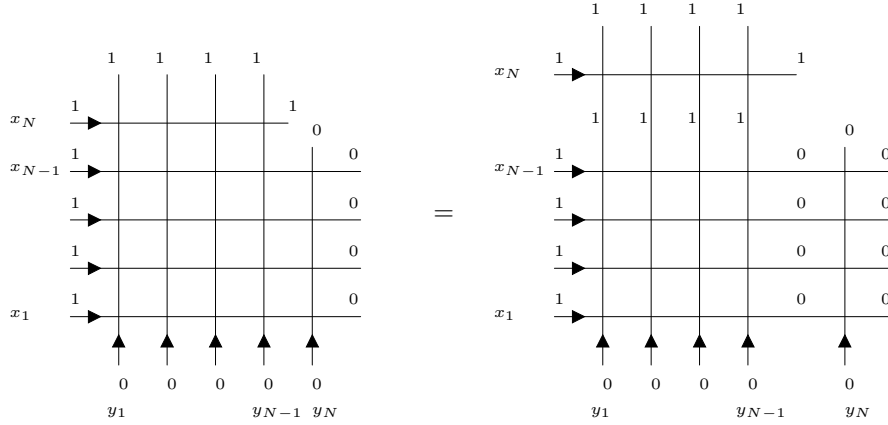


Figure 5: The splitting of the top-right vertex. Setting $x_N = y_N$ makes the DWPF equal to the partition function on the left. The top and right lines give only a trivial contribution, and we obtain the DWPF of one size smaller, as on the right.

This has the graphical interpretation on the left of Figure 4. Using the Yang-Baxter equation the attached vertex may be threaded vertically through the lattice, until it emerges from the top as another a vertex, as on the right of Figure 4. The result of this procedure is the interchange of the lines carrying the rapidities y_j, y_{j+1} . Composing such swaps, one finds the lattice is invariant under any permutation of $\{y_1, \dots, y_N\}$.

C. Setting $x_N = y_N$ forces the top-right vertex in Figure 3 to be a c_- vertex, since b vertices vanish when their incoming rapidities are equal. In addition, this c_- vertex has weight 1, since its rapidities are equal. Therefore the effect of this evaluation is the splitting of the top-right vertex as on the left of Figure 5. Considering the top and right-most lines of the new lattice, it is clear that they only contribute a common factor of a weights to the partition function, which have weight 1. See the right of Figure 5. Neglecting these lines altogether, the remainder of the lattice is the DWPF $Z(\{x\}_{N-1}|\{y\}_{N-1})$. Hence we have proved the recursion relation (8).

D. It is clear from the definition of the vertices in Figure 2 that the DWPF on a 1×1 lattice is a $c_-(x_1, y_1)$ vertex.

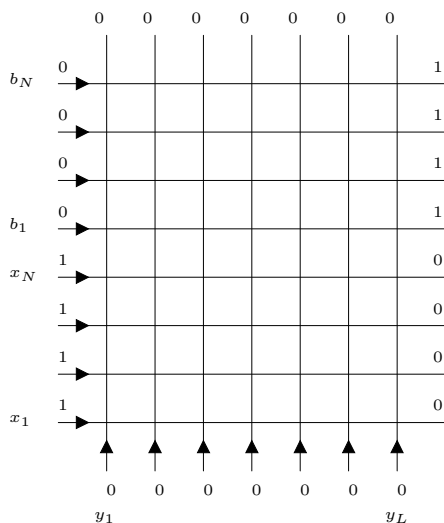


Figure 6: Lattice representation of $S(\{x\}_N, \{b\}_N | \{y\}_L)$. In the algebraic Bethe Ansatz scheme, each horizontal line represents a monodromy matrix operator, see [30]. The vertical lines represent the sites in a spin-chain of length L , with local inhomogeneities.

3.3. Evaluation of the DWPF. Following [28], in the rational parametrization of equation (4) the DWPF is given by

$$(9) \quad Z \left(\{x\}_N | \{y\}_N \right) = \frac{\prod_{i,j=1}^N (x_i - y_j)}{\Delta\{x\}_N \Delta\{-y\}_N} \det \left[\frac{1}{(x_i - y_j)(x_i - y_j + 1)} \right]_{1 \leq i,j \leq N}$$

In the trigonometric parametrization of equation (5) it is given by

$$(10) \quad Z \left(\{x\}_N | \{y\}_N \right) = \frac{e^{|y|-|x|} \prod_{i,j=1}^N [x_i - y_j]}{\Delta\{x\}_N \Delta\{-y\}_N} \det \left[\frac{[\gamma]}{[x_i - y_j][x_i - y_j + \gamma]} \right]_{1 \leq i,j \leq N}$$

where we use the notation $|x| = \sum_{k=1}^N x_k$.

4. A_1 SCALAR PRODUCTS

4.1. The A_1 scalar products in vertex model terms. We have so far discussed the A_1 scalar products in spin-chain terms. We can also consider them in vertex model terms. In vertex model terms, an A_1 scalar product is a partition function $S(\{x\}_N, \{b\}_N | \{y\}_L)$ that depends on two sets of auxiliary variables, or rapidities that flow in horizontal lattice lines, $\{x\}_N = \{x_1, \dots, x_N\}$ and $\{b\}_N = \{b_1, \dots, b_N\}$, and one set of quantum variables, or inhomogeneities that flow in vertical lattice lines, $\{y\}_L = \{y_1, \dots, y_L\}$. If both sets of variables $\{x\}_N$ and $\{b\}_N$ are free, we obtain Korepin's off-shell/off-shell scalar product \mathcal{K}_1 [6]. If the set $\{x\}_N$ is free, while the set $\{b\}_N$ obeys Bethe equations, we obtain Slavnov's off-shell/on-shell scalar product \mathcal{S}_1 [8].

4.2. Definition of the scalar product. In the sequel, we say 'the scalar product' to refer to the A_1 vertex model partition function that evaluates to \mathcal{K}_1 when the set $\{b\}_N$ is free, and to \mathcal{S}_1 when it satisfies Bethe equations.

We define the scalar product $S(\{x\}_N, \{b\}_N | \{y\}_L)$ as the partition function of the lattice configuration in Figure 6.

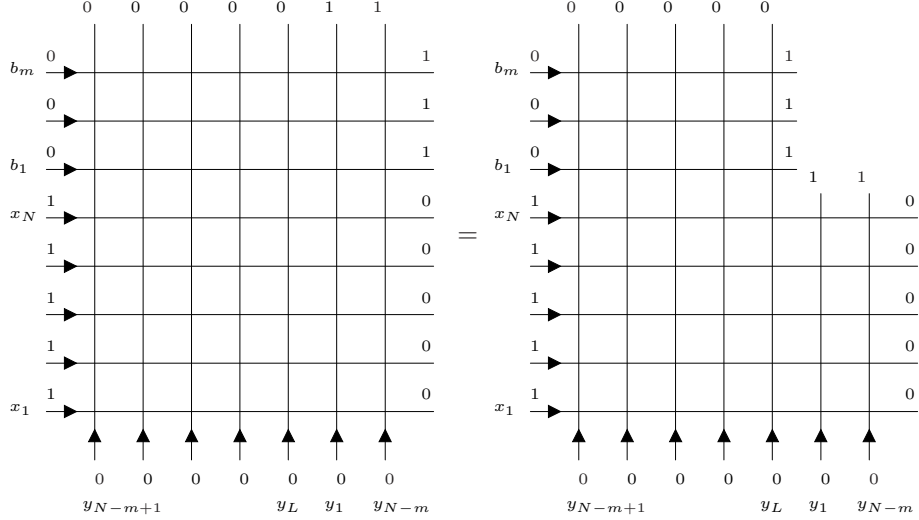


Figure 7: The lattice representation of $S(\{x\}_N, \{b\}_m | \{y\}_L)$ is on the left. The top-right corner of the lattice is constrained to be a product of a vertices, which is why we omit it from the lattice on the right.

More generally, following [29, 30], one can consider a family of related objects called *restricted* scalar products³, denoted $S(\{x\}_N, \{b\}_m | \{y\}_L)$, where $0 \leq m \leq N$. These quantities interpolate between the domain wall partition function $Z(\{x\}_N | \{y\}_N)$, which corresponds to the case $m = 0$, and the full scalar product $\mathcal{S}_1 \equiv S(\{x\}_N, \{b\}_N | \{y\}_L)$ (the case $m = N$). The important point regarding the restricted scalar products is that they are related to each other by a simple recursion relation, see equation (12). The lattice version of a typical restricted scalar product is shown in Figure 7.

4.3. Properties of the A_1 restricted scalar products. Following [30], the A_1 restricted scalar products $S(\{x\}_N, \{b\}_m | \{y\}_L)$ of Section 4.1 satisfy a set of four properties which determine them uniquely.

A. $S(\{x\}_N, \{b\}_m | \{y\}_L)$ is a meromorphic function of the form

$$(11) \quad S \left(\{x\}_N, \{b\}_m \middle| \{y\}_L \right) = \frac{P(\{x\}_N, \{b\}_m | \{y\}_L)}{\prod_{i=1}^N \prod_{j=1}^L (x_i - y_j + 1) \prod_{i=1}^m \prod_{j=N-m+1}^L (b_i - y_j + 1)}$$

where $P(\{x\}_N, \{b\}_m | \{y\}_L)$ is a polynomial of degree $L - N + m - 1$ in b_m .

B. $S(\{x\}_N, \{b\}_m | \{y\}_L)$ is symmetric in the set of variables $\{y_{N-m+1}, \dots, y_L\}$.

C. By setting $b_m = y_{N-m+1}$, we obtain the recursion relation

$$(12) \quad S \left(\{x\}_N, \{b\}_m \middle| \{y\}_L \right) \Big|_{b_m = y_{N-m+1}} = S \left(\{x\}_N, \{b\}_{m-1} \middle| \{y\}_L \right)$$

D. In the case $m = 0$, we have

$$(13) \quad S \left(\{x\}_N, \{b\}_0 \middle| \{y\}_L \right) = \prod_{i=1}^N \prod_{j=N+1}^L \frac{(x_i - y_j)}{(x_i - y_j + 1)} Z \left(\{x\}_N \middle| \{y\}_N \right)$$

³In [30], these were called *intermediate* scalar products. Note that the convention used in this paper is different, in that we restrict the variables $\{b\}_N$ rather than $\{x\}_N$. This is completely permissible, since for now the variables $\{b\}_N$ are free.

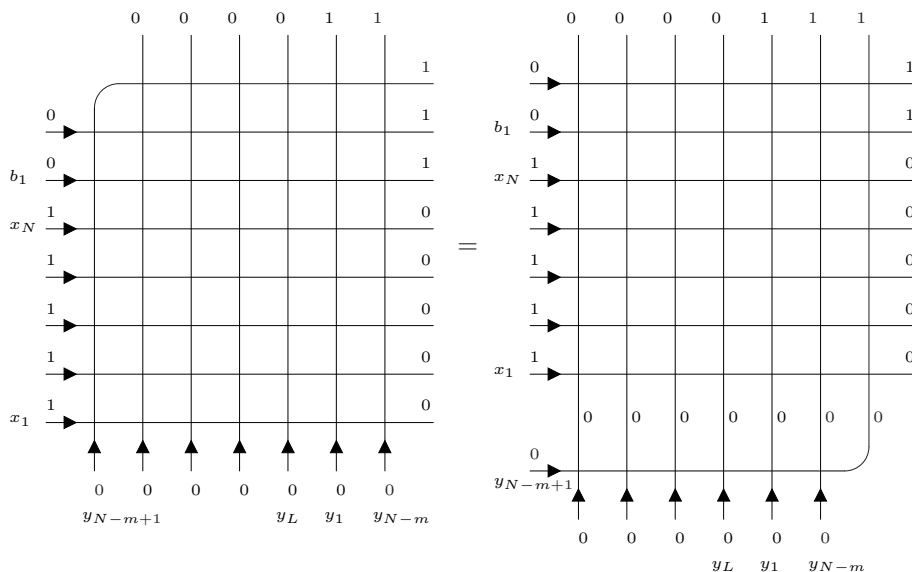


Figure 8: Proving the recursion relation (12). The partition function which results from setting $b_m = y_{N-m+1}$ is on the left. An equivalent version of this partition function, obtained using the Yang-Baxter equation, is on the right. Up to a factor of a weights, the lattice on the right is a restricted scalar product of one size smaller.

Proof. In analogy with Section 3.2, we prove these four properties using the lattice representation of the A_1 restricted scalar product in Figure 7.

A. Referring to the right of Figure 7, we see that all vertices in the bottom N rows contain the factor $\frac{1}{(x_i - y_j + 1)}$, while all those in the top m rows contain $\frac{1}{(b_i - y_j + 1)}$. This explains the denominator of (11), where the size of the second product is smaller than the first due to the non-rectangular geometry of Figure 7. To obtain the numerator, consider the top row of the lattice in Figure 7, which contributes all dependence on the variable b_m . There are $L - N + m$ vertices in this row, and in every configuration exactly one of them is a c_+ vertex, which has degree 0 in b_m . Hence it is clear that $P(\{x\}_N, \{b\}_m | \{y\}_L)$ has degree $L - N + m - 1$ in b_m .

B. To prove the symmetry in $\{y_{N-m+1}, \dots, y_L\}$, one follows the same procedure used to prove property **B** in Section 3.2. Since the argument is identical (albeit applied to a different set of variables), we do not repeat it here.

C. Setting $b_m = y_{N-m+1}$ causes the top-left vertex in Figure 7 to have weight 1, regardless of whether it is an a or c_+ vertex. Since the rapidities on the top and left-most lines are now both y_{N-m+1} , the effect of this evaluation is the same as splitting the top-left vertex as on the left of Figure 8. By repeated application of the Yang-Baxter equation, it is possible to move the curved through the lattice, so that it emerges as on the right of Figure 8. After making this transformation it is clear that (the horizontal part of) the curved line contributes only a common factor of a weights to the overall sum. Hence this part of the line can be neglected, and the remainder of the lattice is simply $S(\{x\}_N, \{b\}_{m-1} | \{y\}_L)$. Hence we have proved the recursion relation (12).

D. In the case $m = 0$, there are no horizontal lines carrying the variables $\{b\}$, and we obtain the lattice shown in Figure 9.

It is straightforward to see that the vertices of the $L - N$ left-most vertical lines are forced to be b vertices. The remaining $N \times N$ block of the lattice is just the DWPF. Hence we immediately obtain the condition (13), which relates the initial restricted scalar product directly to the DWPF.

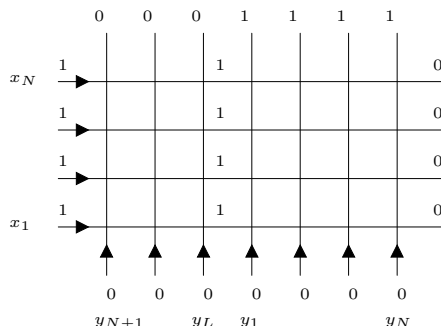


Figure 9: Lattice representation of $S(\{x\}_N, \{b\}_0 | \{y\}_L)$. The left-most $N \times (L - N)$ block is forced to be a product of b vertices, and the remaining part of the lattice is an $N \times N$ DWPF.

4.4. **Evaluation of \mathcal{S}_1 .** Following [8], when the variables $\{b\}_N$ satisfy the Bethe equations

$$(14) \quad \prod_{j \neq i}^N \frac{b_i - b_j + 1}{b_i - b_j - 1} = \prod_{k=1}^L \frac{b_i - y_k + 1}{b_i - y_k}$$

the A_1 scalar product $S(\{x\}_N, \{b\}_N | \{y\}_L)$ can be evaluated in determinant form

$$(15) \quad S \left(\{x\}_N, \{b\}_N \middle| \{y\}_L \right) = \Delta^{-1} \{x\}_N \Delta^{-1} \{-b\}_N \\ \times \det \left[\frac{1}{b_j - x_i} \left(\prod_{k \neq j}^N (b_k - x_i + 1) - \prod_{k \neq j}^N (b_k - x_i - 1) \prod_{k=1}^L \frac{(x_i - y_k)}{(x_i - y_k + 1)} \right) \right]_{1 \leq i, j \leq N}$$

We refer to this special case as *Slavnov's scalar product*, or \mathcal{S}_1 , to distinguish it from the preceding analysis where all variables are considered free.

It is important to remark that a determinant formula can only be found for the scalar product $\mathcal{S}_1 = S(\{x\}_N, \{b\}_N | \{y\}_L)$, depending on the full set of Bethe roots $\{b\}_N$. In particular, we cannot deduce from (15) a determinant formula for (what we defined to be) restricted scalar products $S(\{x\}_N, \{b\}_m | \{y\}_L)$, since these objects arise by treating the set of variables $\{b\}_N$ as free and then restricting them to be equal to inhomogeneities⁴. Nevertheless, we shall only require the determinant formula for $S(\{x\}_N, \{b\}_N | \{y\}_L)$ in what follows, and have introduced restricted scalar products only as a device for uniquely determining $S(\{x\}_N, \{b\}_N | \{y\}_L)$.

5. COLOURING THE A_1 LATTICE CONFIGURATIONS

So far we have considered results related to the A_1 vertex model, and hence all lattice configurations encountered contain only the state variables labelled $\{0, 1\}$. In this and the following sections we remove this restriction, and consider lattice configurations which allow all state variables $\{0, \dots, n\}$ to appear. We call this process *colouring*. The point of these sections is to show that, by colouring the A_1 DWPF and scalar products appropriately, they remain invariant. We describe this invariance by calling the relevant configurations *colour-independent*.

This short section contains identities which are used throughout the rest of the paper, while Sections 6 and 7 study the colouring of the of the DWPF and scalar product, respectively.

5.1. **An identity satisfied by vertex weights.** We shortly make use of the identity

$$(16) \quad 1 = a(x, y) = b_{\pm}(x, y) + c_{\pm}(x, y)$$

which is true for both the rational (4) and trigonometric (5) parametrizations.

⁴In contrast, one can define restricted scalar products $S(\{x\}_m, \{b\}_N | \{y\}_L)$ by restricting the values of the set $\{x\}_N$, which are always free. In this case it is possible to deduce a determinant formula for $S(\{x\}_m, \{b\}_N | \{y\}_L)$, starting from (15), which is explained in [29, 30].

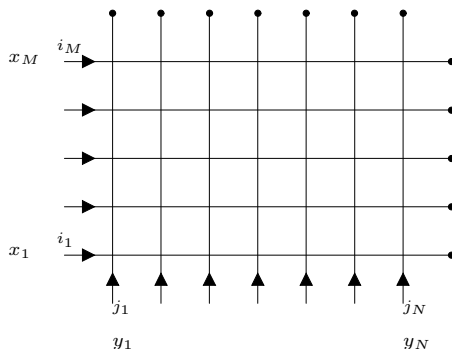


Figure 10: Lattice for the partition function $f_{[i_1, \dots, i_M], [j_1, \dots, j_N]}(\{x\}_M | \{y\}_N)$. Left and bottom boundary segments are fixed to the definite colours shown, while the top and right boundary segments are summed over all values.

5.2. A trivial partition function. Let $f_{[i_1, \dots, i_M], [j_1, \dots, j_N]}(\{x\}_M | \{y\}_N)$ denote the partition function of an $M \times N$ lattice with horizontal rapidities $\{x_1, \dots, x_M\}$ and vertical rapidities $\{y_1, \dots, y_N\}$, whose left and bottom boundary segments are fixed⁵ to colours $\{i_1, \dots, i_M\} \in \{0, 1, \dots, n\}$ and $\{j_1, \dots, j_N\} \in \{0, 1, \dots, n\}$ respectively, while the top and right boundary segments are summed over all colours. We represent this partition function by the lattice shown in Figure 10.

Lemma 1. *For every $M \times N$ lattice and all choices of $\{i_1, \dots, i_M\} \in \{0, 1, \dots, n\}$ and $\{j_1, \dots, j_N\} \in \{0, 1, \dots, n\}$, we have*

$$(17) \quad f_{[i_1, \dots, i_M], [j_1, \dots, j_N]} \left(\{x\}_M | \{y\}_N \right) = 1$$

Proof. Consider the vertex at the top-right corner of Figure 10. For a particular choice of its left and lower incoming colours, k and l respectively, it has the form on the right of Figure 11, see the caption. We conclude that the top-right vertex contributes the weight 1 to the partition function, regardless of its incoming colours. Hence we can ignore its contribution and study the equivalent partition function on the left of Figure 11. Repeating this argument for all vertices in the top row, and then for each subsequent row of the lattice, one ultimately removes all vertices. The statement (17) follows. \square

6. INTRODUCING COLOUR VARIABLES INTO A_1 DOMAIN WALL CONFIGURATIONS

6.1. Colouring the left and top boundaries. Recall the domain wall configuration shown in Figure 3. The bottom and right boundary segments are assigned the colour 0, while the left and top boundary segments are assigned the colour 1. One can think of the colours 1 as black lines which flow into the lattice from the left and exit from the top, while the colours 0 are simply a colourless, or white background.

Let us extend our attention to lattice configurations in an A_n vertex model, where $n \geq 2$, and assume that some or all of the colours which come in from the left take values in $\{2, \dots, n\}$. We denote these left-incoming colours by $\{i_1, \dots, i_N\} \in \{1, 2, \dots, n\}$. Further, assume that the top boundary segments are summed over all possible values in $\{1, 2, \dots, n\}$. We call the

⁵Subsequently, whenever we write $\{k_1, \dots, k_N\} \in \{0, 1, \dots, n\}$, we mean that k_1, \dots, k_N take fixed values in the set $\{0, 1, \dots, n\}$. However, it is *not* true that $\{k_1, \dots, k_N\} \subseteq \{0, 1, \dots, n\}$ since arbitrarily many of the k_i can be equal, and furthermore we say nothing about the relationship between the cardinalities N and $n + 1$.

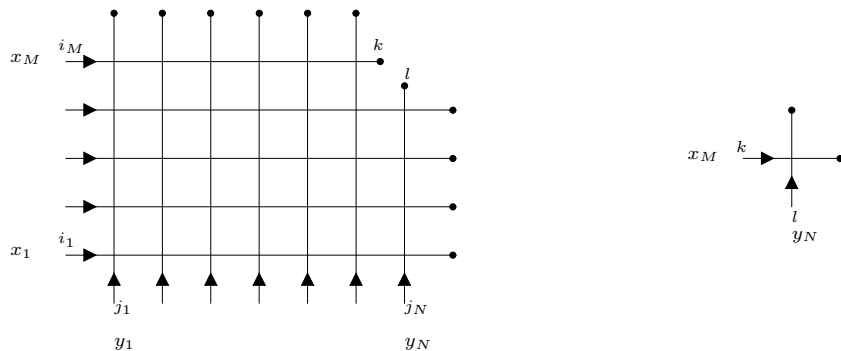


Figure 11: The top-right vertex of the lattice for a particular choice of incoming colours is on the right. When $k = l$, the summation of the top and right segments becomes trivial, and we obtain an $a(x_M, y_N)$ vertex. When $k \neq l$, we use equation (16) to write the sum of vertices as a single $a(x_M, y_N)$ vertex. The lattice which results from the omission of the top-right vertex is on the right. The colours k and l should be considered summed.

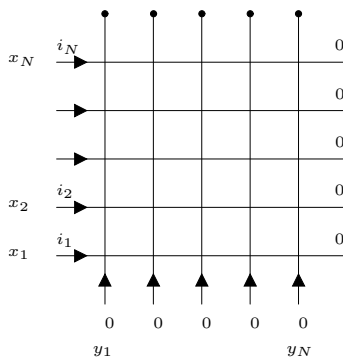


Figure 12: Lattice representation of $Z_{[i_1, \dots, i_N]}(\{x\}_N | \{y\}_N)$. The colours on the left boundary segments are fixed to the definite values $\{i_1, \dots, i_N\} \in \{1, 2, \dots, n\}$, while those on the top boundary segments are summed over all values $\{1, 2, \dots, n\}$, which is indicated by the dots placed on these segments.

resulting lattice a *coloured* domain wall configuration, denoted by $Z_{[i_1, \dots, i_N]}(\{x\}_N | \{y\}_N)$, and represent it as in Figure 12.

Lemma 2. For all choices of introduced colours $\{i_1, \dots, i_N\} \in \{1, 2, \dots, n\}$, we have

$$(18) \quad Z_{[i_1, \dots, i_N]} \left(\{x\}_N | \{y\}_N \right) = Z \left(\{x\}_N | \{y\}_N \right)$$

In other words, the partition function in Figure 12 is colour-independent, and behaves as if all left and top-edge colours were 1, which is a black and white configuration.

Proof. The proof relies on showing that $Z_{[i_1, \dots, i_N]}(\{x\}_N | \{y\}_N)$ satisfies the set of properties A–D in Section 3.2, which uniquely characterize the DWPF.

A. Consider the top row of the lattice in Figure 12, through which x_N flows. Due to the need to conserve the colour $i_N \geq 1$ flowing in from the left, it follows that in every configuration there must be at least one c_- vertex in the top row. As we have already argued in Section 3, this is sufficient to show that

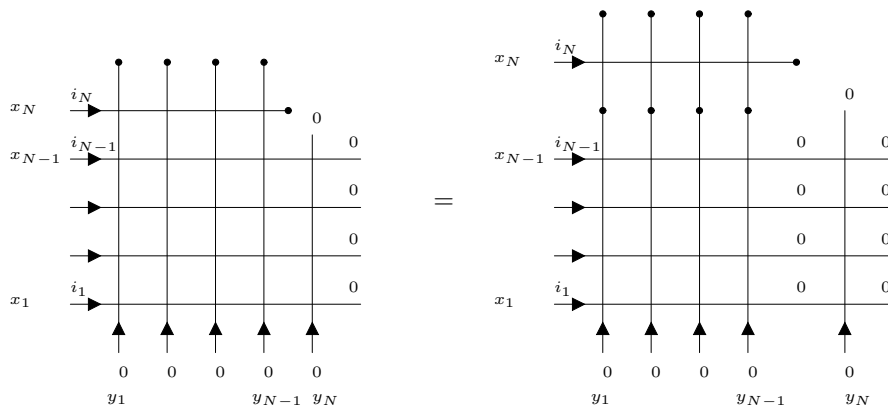


Figure 13: Setting $x_N = y_N$ makes $Z_{[i_1, \dots, i_N]}(\{x\}_N | \{y\}_N)$ equal to the partition function on the left. Due to Lemma 1, the top line of the lattice gives only a trivial contribution to the partition function, and the right line is trivial as before. The remaining part of the lattice, on the right, is $Z_{[i_1, \dots, i_{N-1}]}(\{x\}_{N-1} | \{y\}_{N-1})$.

$$(19) \quad Z_{[i_1, \dots, i_N]} \left(\{x\}_N \middle| \{y\}_N \right) = \frac{P(\{x\}_N | \{y\}_N)}{\prod_{i,j=1}^N (x_i - y_j + 1)}$$

where $P(\{x\}_N | \{y\}_N)$ is a polynomial (maximally) of degree $N - 1$ in x_N .

B. To establish symmetry in $\{y_1, \dots, y_N\}$, one follows the same procedure outlined in Section 3.2. Namely, one attaches an $a(y_{j+1}, y_j)$ vertex at the base of the lattice in Figure 12. Using the Yang-Baxter equation, it is threaded vertically through the lattice until it emerges from the top.

The only difference is that the emerging vertex is not of the type $a(y_{j+1}, y_j)$, rather it is a sum over a $b_{\pm}(y_{j+1}, y_j)$ and $c_{\pm}(y_{j+1}, y_j)$ vertex, due to the summed boundary condition at the top of the lattice. But from (16), such a sum produces an $a(y_{j+1}, y_j)$ vertex. Hence the j -th and $(j + 1)$ -th lattice lines can be freely swapped, and in general the lattice in Figure 12 is invariant under permutations of its vertical lines.

C. Consider the effect of setting $x_N = y_N$ in the lattice in Figure 12. As we have seen before, this removes the possibility that the top-right vertex can be a b vertex and sets the weight of the resultant c_- vertex to 1. Hence the vertex at the intersection of the top and right-most lines splits, and we obtain the lattice on the left of Figure 13. Observe that the right-most line of the lattice contributes a common factor of a vertices to the sum, hence it can be neglected. Similarly, using Lemma 1, the top line of vertices contributes a common factor of 1 to the sum, and can be ignored. We obtain the lattice on the right of Figure 12, which represents $Z_{[i_1, \dots, i_{N-1}]}(\{x\}_{N-1} | \{y\}_{N-1})$. This proves the required recursion relation, namely

$$(20) \quad Z_{[i_1, \dots, i_N]} \left(\{x\}_N \middle| \{y\}_N \right) \Big|_{x_N=y_N} = Z_{[i_1, \dots, i_{N-1}]} \left(\{x\}_{N-1} \middle| \{y\}_{N-1} \right)$$

D. It is easy to check that the correct initial condition is satisfied. Indeed, when $N = 1$, the colour i_1 flowing in from the left must flow out from the top boundary. This constrains the sum on the top boundary to one term only, and we obtain a $c_-(x_1, y_1)$ vertex. \square

7. COLOURING THE A_1 SCALAR PRODUCT CONFIGURATIONS

7.1. Colouring the bottom-left and top-right boundaries. Recall the A_1 scalar product configuration shown in Figure 6. The lower-left and upper-right boundary segments are

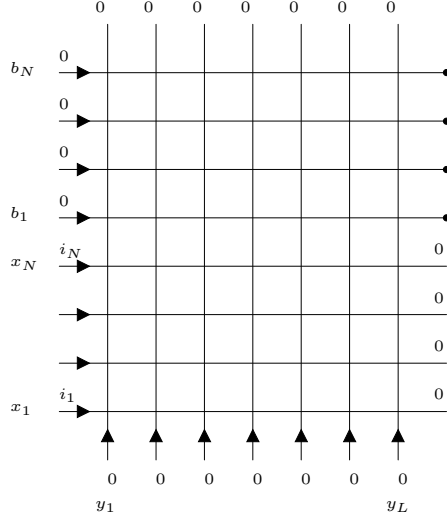


Figure 14: Lattice representation of $S_{[i_1, \dots, i_N]}(\{x\}_N, \{b\}_N | \{y\}_L)$. The colours on the lower-left boundary segments are fixed to the definite values $\{i_1, \dots, i_N\} \in \{1, 2, \dots, n\}$, while those on the upper-right segments are summed over all values $\{1, 2, \dots, n\}$, as indicated by the dots.

assigned the colours 1, which effectively flow in from the bottom-left and exit from the top-right.

In analogy with the previous section, we now generalize to A_n configurations with $n \geq 2$. We assume that some or all of the colours which come in from the lower-left boundary take values in $\{2, \dots, n\}$. As before we denote these incoming colours by $\{i_1, \dots, i_N\} \in \{1, 2, \dots, n\}$. Further, assume that the upper-right boundary segments are summed over all possible values in $\{1, 2, \dots, n\}$. We call the resulting lattice a coloured scalar product configuration, denoted $S_{[i_1, \dots, i_N]}(\{x\}_N, \{b\}_N | \{y\}_L)$, and represent it as in Figure 14. More generally, we can colour the restricted scalar products introduced in Section 4.1. The N lower-left edges are again assigned the fixed values $\{i_1, \dots, i_N\} \in \{1, 2, \dots, n\}$. Summation over all colours $\{1, 2, \dots, n\}$ takes place on the edges in the upper-right corner of the lattice, see Figure 15.

Lemma 3. *For all choices of introduced colours $\{i_1, \dots, i_N\} \in \{1, 2, \dots, n\}$, and $0 \leq m \leq N$, we have*

$$(21) \quad S_{[i_1, \dots, i_N]} \left(\{x\}_N, \{b\}_m | \{y\}_L \right) = S \left(\{x\}_N, \{b\}_m | \{y\}_L \right)$$

In other words, the restricted scalar product in Figure 15 is a colour-independent configuration, and behaves as if its edge colours were the same as those in Figure 7. We emphasize that this result makes no use of the Bethe equations.

Proof. We show that $S_{[i_1, \dots, i_N]}(\{x\}_N, \{b\}_m | \{y\}_L)$ obeys the properties **A–D** in Section 4.1, which uniquely determine the restricted scalar products.

A. Referring to Figure 15 and using Lemma 1, we conclude that the top-right $m \times (N - m)$ block of the lattice contributes a common factor of 1 to the partition function. Therefore we may neglect this part of the lattice, and obtain the configuration on the right of Figure 15. Now the argument proceeds in the same way as the proof of **A** in Section 4.1. Considering the top line of the lattice (whose right edge is summed over all values $\{1, 2, \dots, n\}$), it is clear

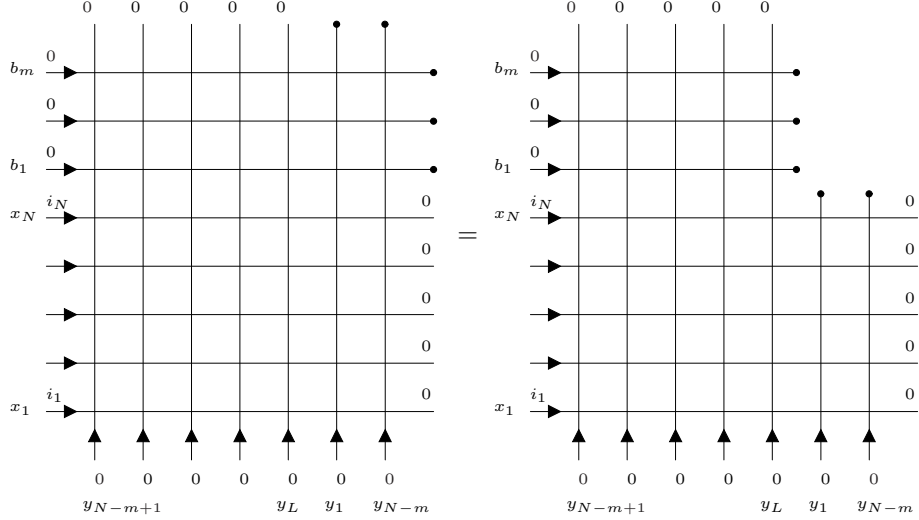


Figure 15: The lattice representation of $S_{[i_1, \dots, i_N]}(\{x\}_N, \{b\}_m | \{y\}_L)$ is on the left. The colours on the lower-left boundary segments are fixed to the definite values $\{i_1, \dots, i_N\} \in \{1, 2, \dots, n\}$, while those on the upper-right segments are summed over all values $\{1, 2, \dots, n\}$, as indicated by the dots. Using Lemma 1, the top-right corner of the lattice gives no contribution to the partition function, and can be neglected as on the right.

that in every term it contains exactly one c_+ vertex. Hence we conclude that

$$(22) \quad S_{[i_1, \dots, i_N]} \left(\{x\}_N, \{b\}_m \middle| \{y\}_L \right) = \frac{P(\{x\}_N, \{b\}_m | \{y\}_L)}{\prod_{i=1}^N \prod_{j=1}^L (x_i - y_j + 1) \prod_{i=1}^m \prod_{j=N-m+1}^L (b_i - y_j + 1)}$$

where $P(\{x\}_N, \{b\}_m | \{y\}_L)$ is a polynomial of degree $L - N + m - 1$ in b_m .

B. Since the edge colours on the left-most $L - N + m$ vertical lines of Figure 15 have fixed value 0 (rather than being summed), the symmetry in $\{y_{N-m+1}, \dots, y_L\}$ is proved by the same argument used to prove **B** in Section 3.2.

C. Setting $b_m = y_{N-m+1}$ in Figure 15 causes the splitting of the top-left vertex, in the same way described in the proof of **C** in Section 4.1. In fact, the argument illustrated by Figure 8 applies here with just a minor change, that each edge 1 colour is replaced by its coloured counterpart. Therefore, one obtains the recursion relation

$$(23) \quad S_{[i_1, \dots, i_N]} \left(\{x\}_N, \{b\}_m \middle| \{y\}_L \right) \Big|_{b_m = y_{N-m+1}} = S_{[i_1, \dots, i_N]} \left(\{x\}_N, \{b\}_{m-1} \middle| \{y\}_L \right)$$

D. In the case $m = 0$, we see that $S_{[i_1, \dots, i_N]}(\{x\}_N, \{b\}_0 | \{y\}_L)$ is represented by the lattice in Figure 16.

Since $i_1, \dots, i_N \geq 1$, by colour-conservation it is clear that these colours pass horizontally through the left-most $L - N$ vertical lines, without interaction. The left $N \times (L - N)$ block of the lattice freezes to a product of b vertices, and the remaining part is the coloured DWPF $Z_{[i_1, \dots, i_N]}(\{x\}_N | \{y\}_N) = Z(\{x\}_N | \{y\}_N)$ (by Lemma 2). Hence

$$(24) \quad S_{[i_1, \dots, i_N]} \left(\{x\}_N, \{b\}_0 \middle| \{y\}_L \right) = \prod_{i=1}^N \prod_{j=N+1}^L \frac{(x_i - y_j)}{(x_i - y_j + 1)} Z \left(\{x\}_N \middle| \{y\}_N \right)$$

□

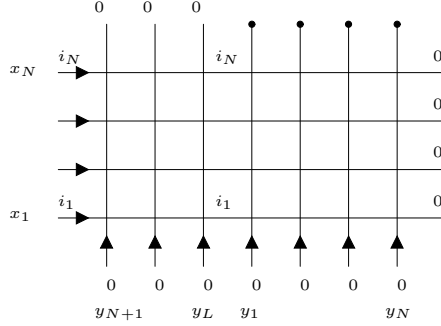


Figure 16: Lattice representation of $S_{[i_1, \dots, i_N]}(\{x\}_N, \{b\}_0 | \{y\}_L)$. Since the colours $\{i_1, \dots, i_N\}$ must be conserved, the left-most $N \times (L - N)$ block is forced to be a product of b vertices. The remaining part of the lattice represents $Z_{[i_1, \dots, i_N]}(\{x\}_N | \{y\}_N)$.

8. A_2 SCALAR PRODUCTS

8.1. Reshetikhin's off-shell/off-shell A_2 scalar product. In [7], Reshetikhin studied scalar products of Bethe vectors in a general class of A_2 quantum integrable models. In this general setup, the Bethe vectors are constructed from $\mathbf{1}$. Elements $t_{ij}(x)$, $i < j$, of the 3×3 monodromy matrix $T_\alpha(x)$, which satisfies the intertwining equation

$$(25) \quad R_{\alpha\beta}^{(2)}(x, y)T_\alpha(x)T_\beta(y) = T_\beta(y)T_\alpha(x)R_{\alpha\beta}^{(2)}(x, y),$$

2. A pseudo-vacuum state $|0\rangle$, which satisfies

$$(26) \quad t_{ii}(x)|0\rangle = a_i(x)|0\rangle, \quad t_{ij}(x)|0\rangle = 0 \text{ for all } i > j,$$

3. The nested Bethe Ansatz for building eigenvectors of the transfer matrix $\mathcal{T}(x) = \sum_{i=1}^3 t_{ii}(x)$. One of the main results in [7] was a sum expression for the off-shell/off-shell scalar product \mathcal{K}_2 , where the dependence on the eigenvalues a_i and the variables of the Bethe vectors was made completely explicit.

In this section we restrict our attention to a particular type of model with A_2 -symmetry, namely, a spin chain whose monodromy matrix is constructed from a product of fundamental and anti-fundamental representations of the universal R -matrix,

$$(27) \quad T_\alpha(x) = R_{\alpha 1}^{(2)}(x, y_1) \dots R_{\alpha L}^{(2)}(x, y_L) R_{\alpha 1^*}^{*(2)}(x, z_1) \dots R_{\alpha M^*}^{*(2)}(x, z_M)$$

where

$$(28) \quad R_{\alpha i}^{(2)}(x, y_i) \in \text{End}(V_\alpha \otimes V_i), \quad R_{\alpha i^*}^{*(2)}(x, z_i) = \left(R_{\alpha i^*}^{(2)}(-x, -z_i) \right)^{t_{i^*}} \in \text{End}(V_\alpha \otimes V_{i^*})$$

and where we use an asterisk to label the second set of quantum spaces, V_{i^*} , to distinguish them from the first set V_i . This particular model was also considered in [7], where it played a central role in calculating the off-shell/off-shell scalar product \mathcal{K}_2 . Our goal is to use the arguments developed earlier in the paper to study the scalar product of this model, by representing it as the partition function of a certain lattice configuration.

8.2. Two versions of the off-shell/on-shell scalar product \mathcal{S}_2 . For a detailed discussion of the construction of \mathcal{S}_2 for the model (27), we refer the reader to [7]. Here we shall use the results of [7] without further explanation. Once again, we use the term ‘scalar product’ to indicate the partition function of certain configurations in the A_2 vertex model. In A_2 vertex model terms, the scalar product

$$(29) \quad \mathcal{S}_2 \equiv S \left(\{x^{(2)}\}, \{x^{(1)}\}, \{b^{(1)}\}, \{b^{(2)}\} \middle| \{y\}, \{z\} \right) = \left\langle \{x^{(2)}\}, \{x^{(1)}\} \middle| \{b^{(1)}\}, \{b^{(2)}\} \right\rangle$$

depends on six sets of variables. $\{x^{(1)}\} = \{x_1^{(1)}, \dots, x_\ell^{(1)}\}$ and $\{x^{(2)}\} = \{x_1^{(2)}, \dots, x_m^{(2)}\}$ are free auxiliary rapidities, $\{b^{(1)}\} = \{b_1^{(1)}, \dots, b_\ell^{(1)}\}$ and $\{b^{(2)}\} = \{b_1^{(2)}, \dots, b_m^{(2)}\}$ are auxiliary

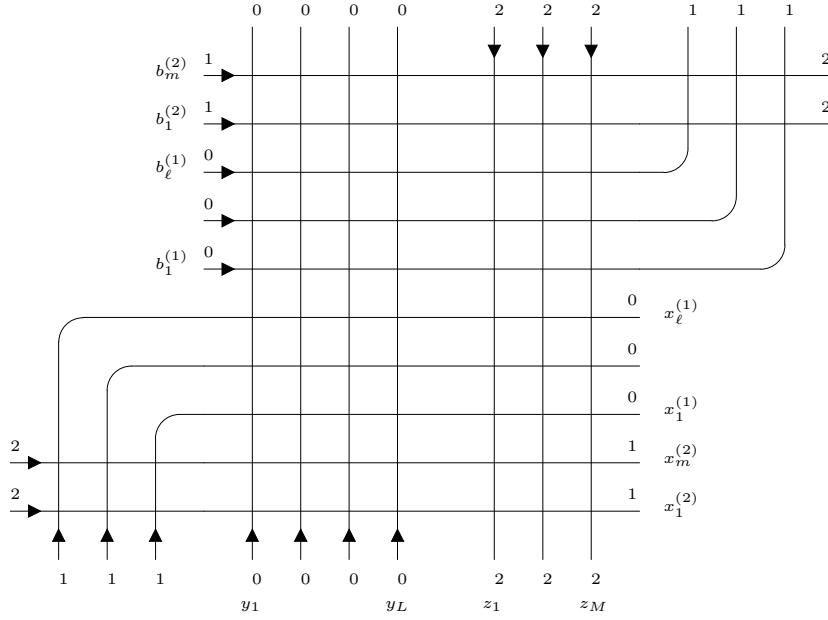


Figure 17: First lattice representation of $S(\{x^{(2)}\}, \{x^{(1)}\}, \{b^{(1)}\}, \{b^{(2)}\} | \{y\}, \{z\})$.

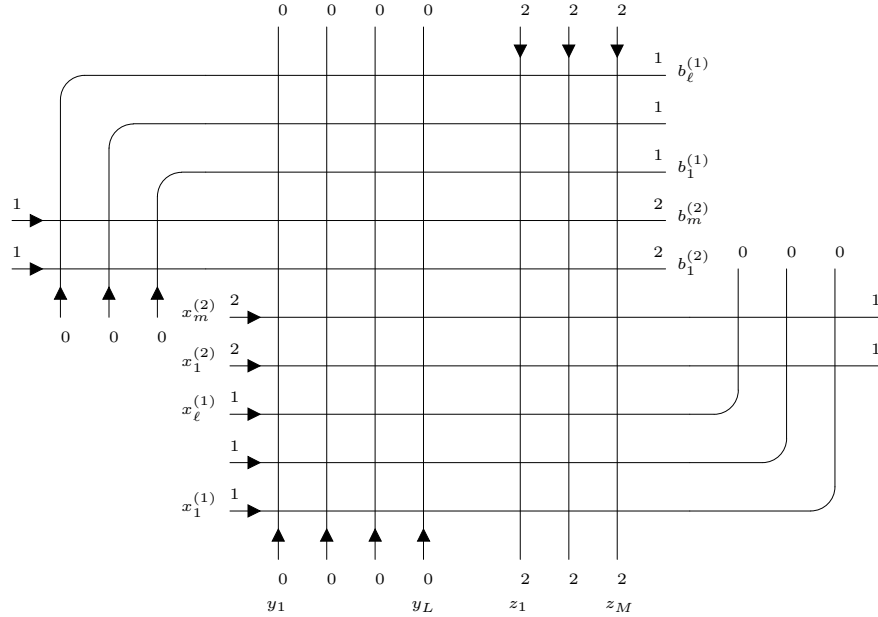


Figure 18: Second lattice representation of $S(\{x^{(2)}\}, \{x^{(1)}\}, \{b^{(1)}\}, \{b^{(2)}\} | \{y\}, \{z\})$.

rapidities which satisfy Bethe equations, and $\{y\} = \{y_1, \dots, y_L\}$ and $\{z\} = \{z_1, \dots, z_M\}$ are quantum rapidities. In order for the scalar product to be non-zero, we require that the cardinalities satisfy $\ell + m \leq L + M$. The scalar product is the partition function of the lattice shown in Figure 17. Using the Yang-Baxter equation repeatedly, the lattice in Figure 17 can be transformed to that shown in Figure 18.

Despite recent studies [2, 26, 27, 31, 32], no compact expression for \mathcal{S}_2 , such as a determinant, is known to exist, unless the variables $\{x^{(1)}\}$ and $\{x^{(2)}\}$ also satisfy Bethe equations

[7, 27]. Alternatively, one can consider the case where the Bethe eigenvector in \mathcal{S}_2 becomes an A_1 -like Bethe eigenvector, which amounts to sending one set of Bethe variables to infinity. While less than fully general, this case is relevant to studies of 3-point functions that involve operators from an A_2 sub-sector of SYM_4 . We consider this case in the rest of this section, with the aim of recovering the results of [2] from a vertex-model point of view.

We treat the partition functions in Figures 17 and 18 as equivalent expressions for the A_2 scalar product. When we send $\{b^{(2)}\} \rightarrow \{\infty\}$, we find it most useful to start from the representation in Figure 17. Conversely, when we send $\{b^{(1)}\} \rightarrow \{\infty\}$, we start from the representation in Figure 18.

8.3. Bethe equations. As we have already mentioned, in this section we assume that $\{b^{(1)}\}$ and $\{b^{(2)}\}$ are Bethe roots at all times. To be precise, we assume that they are solutions of the nested Bethe Ansatz equations, which for the model under consideration are given by

$$(30) \quad \prod_{j \neq i}^{\ell} \frac{b_i^{(1)} - b_j^{(1)} + 1}{b_i^{(1)} - b_j^{(1)} - 1} = \prod_{j=1}^L \frac{b_i^{(1)} - y_j + 1}{b_i^{(1)} - y_j} \prod_{k=1}^m \frac{b_i^{(1)} - b_k^{(2)}}{b_i^{(1)} - b_k^{(2)} - 1}$$

$$(31) \quad \prod_{j \neq i}^m \frac{b_i^{(2)} - b_j^{(2)} + 1}{b_i^{(2)} - b_j^{(2)} - 1} = \prod_{j=1}^M \frac{b_i^{(2)} - z_j}{b_i^{(2)} - z_j - 1} \prod_{k=1}^{\ell} \frac{b_i^{(2)} - b_k^{(1)} + 1}{b_i^{(2)} - b_k^{(1)}}$$

When we take the limit in which a set of Bethe roots $\{b^{(1)}\}$ or $\{b^{(2)}\}$ tends to infinity, this causes a simplification of the Bethe equations (30) and (31). Namely, in this limit, one set of equations trivializes and the remaining set becomes of A_1 -type. We obtain

$$(32) \quad \prod_{j \neq i}^{\ell} \frac{b_i^{(1)} - b_j^{(1)} + 1}{b_i^{(1)} - b_j^{(1)} - 1} = \prod_{j=1}^L \frac{b_i^{(1)} - y_j + 1}{b_i^{(1)} - y_j}, \quad \text{when } \{b^{(2)}\} \rightarrow \{\infty\}$$

$$(33) \quad \prod_{j \neq i}^m \frac{b_i^{(2)} - b_j^{(2)} + 1}{b_i^{(2)} - b_j^{(2)} - 1} = \prod_{j=1}^M \frac{b_i^{(2)} - z_j}{b_i^{(2)} - z_j - 1}, \quad \text{when } \{b^{(1)}\} \rightarrow \{\infty\}$$

Equations (32) are precisely the Bethe equations (14) for an A_1 XXX spin chain built entirely from fundamental representations of the universal R -matrix, while (33) are those for a spin chain built entirely from anti-fundamental representations.

8.4. Change of normalization. In this section it is most convenient to use the normalization in which the b weights are equal to 1, rather than the a weights. Specifically, we assume that

$$(34) \quad a(x, y) = \frac{x - y + 1}{x - y}, \quad b(x, y) = 1, \quad c(x, y) = \frac{1}{x - y}$$

All formulae which we use from previous sections, which were based on the normalization with $a(x, y) = 1$, must be renormalized appropriately.

8.5. Trivializing the $\{b^{(2)}\}$ lines. Let us define

$$(35) \quad S \left(\{x^{(2)}\}, \{x^{(1)}\}, \{b^{(1)}\}, \{\infty\} \middle| \{y\}, \{z\} \right) = \frac{1}{m!} \lim_{\{b^{(2)}\} \rightarrow \{\infty\}} \left(b_m^{(2)} \dots b_1^{(2)} S \left(\{x^{(2)}\}, \{x^{(1)}\}, \{b^{(1)}\}, \{b^{(2)}\} \middle| \{y\}, \{z\} \right) \right)$$

Lemma 4. $S(\{x^{(2)}\}, \{x^{(1)}\}, \{b^{(1)}\}, \{\infty\} | \{y\}, \{z\})$ is equal to the partition function shown in Figure 20.

Proof. We start from the representation of the scalar product in Figure 17. Using the Yang-Baxter equation and deleting all frozen blocks of b vertices, we transform the top half of the lattice to the form in Figure 19.

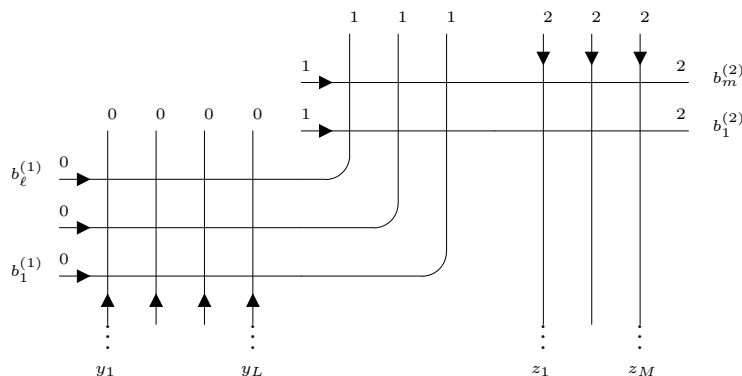


Figure 19: Top half of the scalar product, modified using the Yang-Baxter equation.

Consider sending $b_m^{(2)}, \dots, b_1^{(2)}$ to infinity, one at a time. $b_m^{(2)}$ corresponds to the top horizontal line of Figure 19, and we are interested in the possible positions of c vertices along this line. The c vertices are positioned either at the intersection of the $(b_m^{(2)}, b_i^{(1)})$ lines or the $(z_i, b_m^{(2)})$ lines. Let us refer to a c vertex of the type $1/(b_m^{(2)} - b_i^{(1)})$ as a *left* c vertex, and a c vertex of the type $1/(z_i - b_m^{(2)})$ as a *right* c vertex.

Evidently, in the limit being taken the only configurations which contribute are those which have one c vertex occurring in the top horizontal line. This rules out the possibility of the colour 0 entering this line, to leading order. Hence if we multiply by $b_m^{(2)}$ and take the limit $b_m^{(2)} \rightarrow \infty$, we trivialize the top line and produce a sum over the colours $\{1, 2\}$ along the top of the lattice, such that **1**. The colours $\{\alpha_1, \dots, \alpha_\ell\}$ along the top left are summed over $\{1, 2\}$ with exactly one $\alpha_k = 2$, and all colours $\{\beta_1, \dots, \beta_M\}$ along the top right are equal to 2 (and the configuration is not weighted by a minus sign, because it comes from a left c vertex), or **2**. All colours $\{\alpha_1, \dots, \alpha_\ell\}$ along the top left are equal to 1, and the colours $\{\beta_1, \dots, \beta_M\}$ along the top right are summed over $\{1, 2\}$ with exactly one $\beta_k = 1$ (and the configuration is weighted by a minus sign, because it comes from a right c vertex).

It is easy to see that by repeating this procedure over all $\{b^{(2)}\}$, we trivialize this upper block of vertices and arrive at the configuration shown in Figure 20, with precisely the sum indicated in the caption. Notice that the factor $1/m!$ eliminates multiple-countings which arise from the successive limits. □

8.6. Partitioning of $S(\{x^{(2)}\}, \{x^{(1)}\}, \{b^{(1)}\}, \{\infty\} | \{y\}, \{z\})$. Studying Figure 20, from colour conservation arguments the colours 0 entering at the base of the lattice give a product of b weights, arising from the intersection with the lowest m horizontal lines. Since the b weights have weight 1, we obtain

$$(36) \quad S \left(\{x^{(2)}\}, \{x^{(1)}\}, \{b^{(1)}\}, \{\infty\} | \{y\}, \{z\} \right) = \sum_{Z_{[i_\ell, \dots, i_1], [j_1, \dots, j_M]}} \left(\{x^{(2)}\} | \{x^{(1)}\}, \{z\} \right) S_{[i_1, \dots, i_\ell], [j_1, \dots, j_M]} \left(\{x^{(1)}\}, \{b^{(1)}\} | \{y\}, \{z\} \right)$$

where the sum is over all sets of integers $\{i_1, \dots, i_\ell\}, \{j_1, \dots, j_M\}$ taking values in $\{1, 2\}$, such that $\#(i_k = 2) + \#(j_k = 1) = m$.

$Z_{[i_\ell, \dots, i_1], [j_1, \dots, j_M]}(\{x^{(2)}\} | \{x^{(1)}\}, \{z\})$ and $S_{[i_1, \dots, i_\ell], [j_1, \dots, j_M]}(\{x^{(1)}\}, \{b^{(1)}\} | \{y\}, \{z\})$ are the partition functions on the left and right of Figure 21, respectively.

8.7. Colour-independence of $S_{[i_1, \dots, i_\ell], [j_1, \dots, j_M]}(\{x^{(1)}\}, \{b^{(1)}\} | \{y\}, \{z\})$.

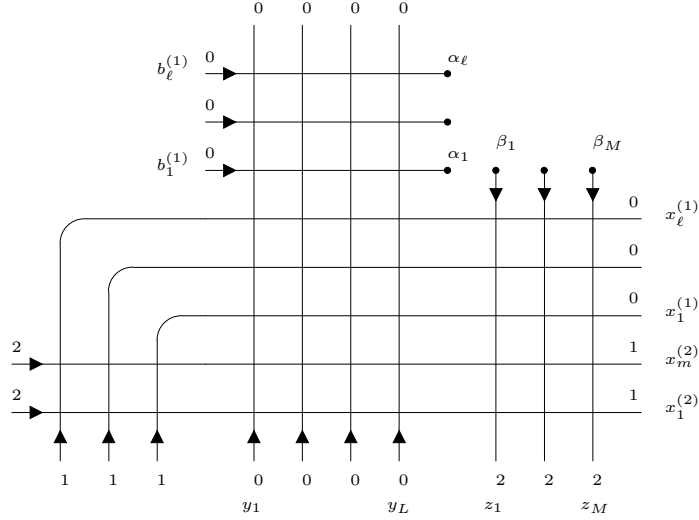


Figure 20: Lattice representation of $S(\{x^{(2)}\}, \{x^{(1)}\}, \{b^{(1)}\}, \{\infty\} | \{y\}, \{z\})$. The points marked $\{\alpha_1, \dots, \alpha_\ell, \beta_1, \dots, \beta_M\}$ are summed over the colours $\{1, 2\}$, such that $\#(\alpha_k = 2) + \#(\beta_k = 1) = m$. There is a multiplicative minus sign for every $\beta_k = 1$.

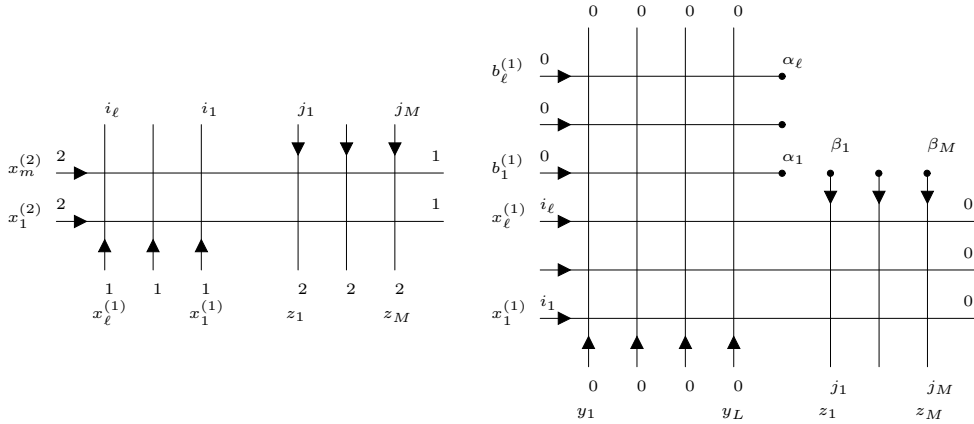


Figure 21: The partition function $Z_{[i_\ell, \dots, i_1], [j_1, \dots, j_M]}(\{x^{(2)}\} | \{x^{(1)}\}, \{z\})$ is on the left. The partition function $S_{[i_1, \dots, i_\ell], [j_1, \dots, j_M]}(\{x^{(1)}\}, \{b^{(1)}\} | \{y\}, \{z\})$ is on the right.

Lemma 5. For all fixed choices of $\{i_1, \dots, i_\ell\}, \{j_1, \dots, j_M\}$ such that $\#(i_k = 2) + \#(j_k = 1) = m$, we have

$$(37) \quad S_{[i_1, \dots, i_\ell], [j_1, \dots, j_M]} \left(\{x^{(1)}\}, \{b^{(1)}\} | \{y\}, \{z\} \right) = (-)^{\#(j_k=1)} S \left(\{x^{(1)}\}, \{b^{(1)}\} | \{y\} \right)$$

where the right hand side of (37) is an A_1 scalar product of the type in Figure 6.

Proof. We consider the colours $\{\beta_1, \dots, \beta_M\}$ which enter the right part of the lattice. Since none of these colours are equal to 0, by colour-conservation we find that $\beta_k = j_k$ for all $1 \leq k \leq M$. This trivializes the sum over $\{\beta_1, \dots, \beta_M\}$ and constrains the right part of the lattice to be a product of b weights. We also pick up the multiplicative sign $(-)^{\#(\beta_k=1)} = (-)^{\#(j_k=1)}$.

It follows that $S_{[i_1, \dots, i_\ell], [j_1, \dots, j_M]}(\{x^{(1)}\}, \{b^{(1)}\} | \{y\}, \{z\})$ does not genuinely depend on $\{z\}$, and the left part of the lattice is a coloured scalar product of the type in Figure 14. As we have already seen, this coloured scalar product is colour-invariant, and equal to $S(\{x^{(1)}\}, \{b^{(1)}\} | \{y\})$.

□

Returning to the sum (36), $S_{[i_1, \dots, i_\ell], [j_1, \dots, j_M]}(\{x^{(1)}\}, \{b^{(1)}\}|\{y\}, \{z\})$ is virtually a constant with respect to the summation, since $S(\{x^{(1)}\}, \{b^{(1)}\}|\{y\})$ is a common factor to all terms. Therefore we turn to computing $\sum(-)^{\#(j_k=1)} Z_{[i_\ell, \dots, i_1], [j_1, \dots, j_M]}(\{x^{(2)}\}|\{x^{(1)}\}, \{z\})$, which is described in the next subsection.

8.8. Calculation of $\sum(-)^{\#(j_k=1)} Z_{[i_\ell, \dots, i_1], [j_1, \dots, j_M]}(\{x^{(2)}\}|\{x^{(1)}\}, \{z\})$. We write

$$(38) \quad \sum(-)^{\#(j_k=1)} Z_{[i_\ell, \dots, i_1], [j_1, \dots, j_M]} \left(\{x^{(2)}\} \middle| \{x^{(1)}\}, \{z\} \right) = \frac{1}{m!} \lim_{\{b^{(2)}\} \rightarrow \{\infty\}} \left(b_m^{(2)} \dots b_1^{(2)} S \left(\{x^{(2)}\}, \{b^{(2)}\} \middle| \{x^{(1)}\}, \{z\} \right) \right)$$

where the right hand side of (38) is the degeneration of an A_1 scalar product. Full details are provided in Appendix **A**, where the right hand side is expressed in determinant form. Observe that we have reintroduced the variables $\{b^{(2)}\}$ for purely aesthetic reasons, and could have called them anything since they are dummy variables.

8.9. Factorization of $S(\{x^{(2)}\}, \{x^{(1)}\}, \{b^{(1)}\}, \{\infty\}|\{y\}, \{z\})$. Combining the results (37) and (38), we see that (36) can be evaluated as

$$(39) \quad S \left(\{x^{(2)}\}, \{x^{(1)}\}, \{b^{(1)}\}, \{\infty\} \middle| \{y\}, \{z\} \right) = S \left(\{x^{(1)}\}, \{b^{(1)}\} \middle| \{y\} \right) \frac{1}{m!} \lim_{\{b^{(2)}\} \rightarrow \{\infty\}} \left(b_m^{(2)} \dots b_1^{(2)} S \left(\{x^{(2)}\}, \{b^{(2)}\} \middle| \{x^{(1)}\}, \{z\} \right) \right)$$

where both factors are A_1 scalar products, or a degeneration thereof. Due to the Bethe equations in the $\{b^{(2)}\} \rightarrow \{\infty\}$ regime (32), the first factor can be evaluated as a Slavnov determinant. The second factor is also a determinant, given by equation (52) in Appendix **A**. Putting these results together, we obtain

$$(40) \quad S \left(\{x^{(2)}\}, \{x^{(1)}\}, \{b^{(1)}\}, \{\infty\} \middle| \{y\}, \{z\} \right) = \Delta^{-1} \{x^{(1)}\} \Delta^{-1} \{-b^{(1)}\} \Delta^{-1} \{x^{(2)}\} \times \det \left(\frac{1}{b_j^{(1)} - x_i^{(1)}} \left(\prod_{k \neq j}^{\ell} (b_k^{(1)} - x_i^{(1)} + 1) \prod_{k=1}^L \left(\frac{x_i^{(1)} - y_k + 1}{x_i^{(1)} - y_k} \right) - \prod_{k \neq j}^{\ell} (b_k^{(1)} - x_i^{(1)} - 1) \right) \right)_{1 \leq i, j \leq \ell} \times \det \left((x_i^{(2)})^{j-1} \prod_{k=1}^{\ell} \left(\frac{x_i^{(2)} - x_k^{(1)} + 1}{x_i^{(2)} - x_k^{(1)}} \right) - (x_i^{(2)} + 1)^{j-1} \prod_{k=1}^M \left(\frac{x_i^{(2)} - z_k - 1}{x_i^{(2)} - z_k} \right) \right)_{1 \leq i, j \leq m}$$

This formula is the A_2 vertex-model version of equation (106) in [2]. Here we have given a derivation based purely on colour-independence in coloured vertex model partition functions.

8.10. Trivializing the $\{b^{(1)}\}$ lines. The second half of this section is devoted to taking the other limit, $\{b^{(1)}\} \rightarrow \{\infty\}$. Let us define

$$(41) \quad S \left(\{x^{(2)}\}, \{x^{(1)}\}, \{\infty\}, \{b^{(2)}\} \middle| \{y\}, \{z\} \right) = \frac{1}{\ell!} \lim_{\{b^{(1)}\} \rightarrow \{\infty\}} \left(b_\ell^{(1)} \dots b_1^{(1)} S \left(\{x^{(2)}\}, \{x^{(1)}\}, \{b^{(1)}\}, \{b^{(2)}\} \middle| \{y\}, \{z\} \right) \right)$$

Lemma 6. $S(\{x^{(2)}\}, \{x^{(1)}\}, \{\infty\}, \{b^{(2)}\}|\{y\}, \{z\})$ is equal to the partition function shown in Figure 22.

Proof. The proof is similar in nature to the proof of Lemma 4. This time we start from the representation of the scalar product in Figure 18, with its top half modified as in Figure 19.

Consider sending $b_\ell^{(1)}, \dots, b_1^{(1)}$ to infinity, one at a time. $b_\ell^{(1)}$ corresponds to the top-most of the $\{b^{(1)}\}$ lines, and we are interested in the possible positions of c vertices along this line. The c vertices are positioned either at the intersection of the $(b_\ell^{(1)}, y_i)$ lines or the $(b_i^{(2)}, b_\ell^{(1)})$

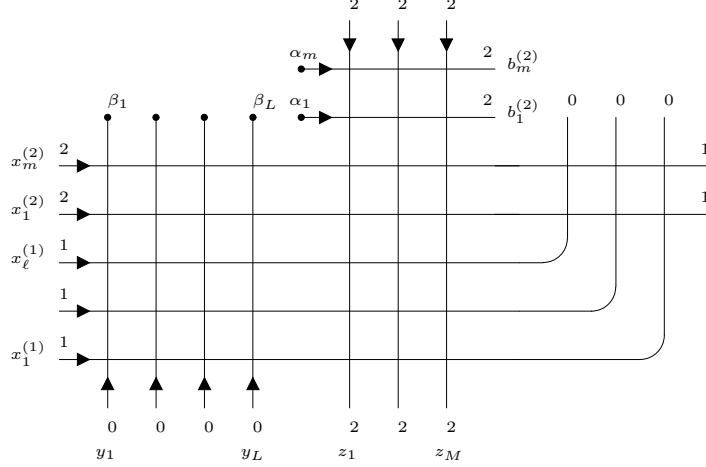


Figure 22: Lattice representation of $S(\{x^{(2)}\}, \{x^{(1)}\}, \{\infty\}, \{b^{(2)}\} | \{y\}, \{z\})$. The points marked $\{\alpha_1, \dots, \alpha_m, \beta_1, \dots, \beta_L\}$ are summed over the colours $\{0, 1\}$, such that $\#(\alpha_k = 0) + \#(\beta_k = 1) = \ell$. There is a multiplicative minus sign for every $\alpha_k = 0$.

lines. We refer to a c vertex of the type $1/(b_\ell^{(1)} - y_i)$ as a left c vertex, and a c vertex of the type $1/(b_i^{(2)} - b_\ell^{(1)})$ as a right c vertex.

In the limit being taken, the only configurations which contribute are those which have a single c vertex occurring along this line. This eliminates the possibility of the colour 2 entering this line, to leading order. Hence if we multiply by $b_\ell^{(1)}$ and take the limit $b_\ell^{(1)} \rightarrow \infty$, we trivialize this line and produce a sum over the colours $\{0, 1\}$ along the edge that the line formerly occupied, such that **1**. All colours $\{\alpha_1, \dots, \alpha_m\}$ are equal to 1, and the colours $\{\beta_1, \dots, \beta_L\}$ are summed over $\{0, 1\}$ with exactly one $\beta_k = 1$ (and the configuration is not weighted by a minus sign, because it comes from a left c vertex), or **2**. The colours $\{\alpha_1, \dots, \alpha_m\}$ are summed over $\{0, 1\}$ with exactly one $\alpha_k = 0$, and all colours $\{\beta_1, \dots, \beta_L\}$ are equal to 0 (and the configuration is weighted by a minus sign, because it comes from a right c vertex).

Repeating this procedure over all $\{b^{(1)}\}$, we ultimately arrive at the configuration shown in Figure 22, with precisely the sum indicated in the caption. The factor $1/\ell!$ compensates for multiple-countings which arise from the successive limits. \square

8.11. Partitioning of $S(\{x^{(2)}\}, \{x^{(1)}\}, \{\infty\}, \{b^{(2)}\} | \{y\}, \{z\})$. Studying Figure 22, by colour-conservation arguments the colours 2 leaving at the base of the lattice give rise to a product of b weights, arising from the intersection with the lowest ℓ horizontal lines. Since the b weights have weight 1, we obtain

$$(42) \quad S \left(\{x^{(2)}\}, \{x^{(1)}\}, \{\infty\}, \{b^{(2)}\} \middle| \{y\}, \{z\} \right) = \sum_{S_{[j_1, \dots, j_L], [i_1, \dots, i_m]}} \left(\{x^{(2)}\}, \{b^{(2)}\} \middle| \{y\}, \{z\} \right) Z_{[j_1, \dots, j_L], [i_1, \dots, i_m]} \left(\{x^{(1)}\} \middle| \{y\}, \{x^{(2)}\} \right)$$

where the sum is over all sets of integers $\{j_1, \dots, j_L\}, \{i_1, \dots, i_m\}$ taking values in $\{0, 1\}$, such that $\#(i_k = 0) + \#(j_k = 1) = \ell$. $S_{[j_1, \dots, j_L], [i_1, \dots, i_m]}(\{x^{(2)}\}, \{b^{(2)}\} | \{y\}, \{z\})$ and $Z_{[j_1, \dots, j_L], [i_1, \dots, i_m]}(\{x^{(1)}\} | \{y\}, \{x^{(2)}\})$ are the partition functions on the left and right of Figure 23, respectively.

8.12. Colour-independence of $S_{[j_1, \dots, j_L], [i_1, \dots, i_m]}(\{x^{(2)}\}, \{b^{(2)}\} | \{y\}, \{z\})$.

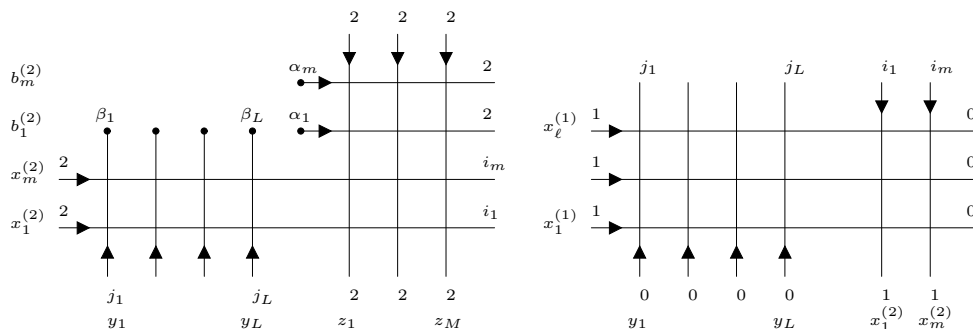


Figure 23: The partition function $S_{[j_1, \dots, j_L], [i_1, \dots, i_m]}(\{x^{(2)}\}, \{b^{(2)}\} | \{y\}, \{z\})$ is on the left. The partition function $Z_{[j_1, \dots, j_L], [i_1, \dots, i_m]}(\{x^{(1)}\} | \{y\}, \{x^{(2)}\})$ is on the right.

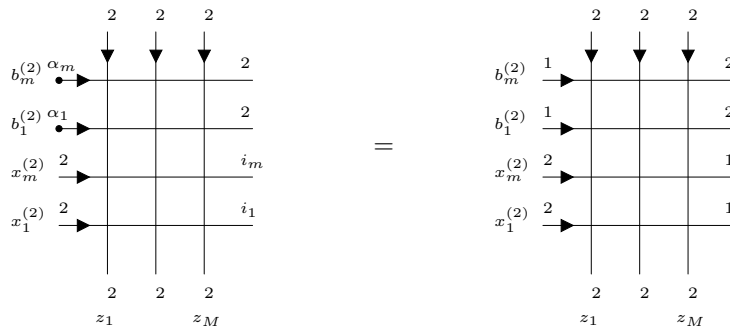


Figure 24: Shown on the left hand side, the coloured scalar product configuration which $S_{[j_1, \dots, j_L], [i_1, \dots, i_m]}(\{x^{(2)}\}, \{b^{(2)}\} | \{y\}, \{z\})$ reduces to. This configuration turns out to be colour-invariant, and equal to the A_1 scalar product $S(\{x^{(2)}\}, \{b^{(2)}\} | \emptyset, \{z\})$ on the right hand side.

Lemma 7. For all fixed choices of $\{j_1, \dots, j_L\}, \{i_1, \dots, i_m\}$ such that $\#(i_k = 0) + \#(j_k = 1) = \ell$, we have

$$(43) \quad S_{[j_1, \dots, j_L], [i_1, \dots, i_m]}(\{x^{(2)}\}, \{b^{(2)}\} | \{y\}, \{z\}) = (-)^{\#(i_k=0)} S(\{x^{(2)}\}, \{b^{(2)}\} | \emptyset, \{z\})$$

where the right hand side of (43) is the A_1 scalar product on the right of Figure 24.

Proof. We consider the colours $\{\beta_1, \dots, \beta_L\}$ which leave from the left part of the lattice. Since none of these colours are equal to 2, by colour-conservation we find that $\beta_k = j_k$ for all $1 \leq k \leq L$. This trivializes the sum over $\{\beta_1, \dots, \beta_L\}$ and constrains the left part of the lattice to be a product of b weights.

It follows that $S_{[j_1, \dots, j_L], [i_1, \dots, i_m]}(\{x^{(2)}\}, \{b^{(2)}\} | \{y\}, \{z\})$ does not genuinely depend on $\{y\}$, and the right part of the lattice is equal to the coloured scalar product on the left of Figure 24. Although we do not prove it here, this coloured scalar product is colour-invariant and equal to $S(\{x^{(2)}\}, \{b^{(2)}\} | \emptyset, \{z\})$, on the right of Figure 24. A minus sign of $(-)^{\#(i_k=0)} = (-)^{\#(i_k=0)}$ is remnant from the limit $\{b^{(1)}\} \rightarrow \{\infty\}$, taken earlier. \square

Returning to the sum (42), $S_{[j_1, \dots, j_L], [i_1, \dots, i_m]}(\{x^{(2)}\}, \{b^{(2)}\} | \{y\}, \{z\})$ is effectively constant with respect to the summation, since we can extract $S(\{x^{(2)}\}, \{b^{(2)}\} | \emptyset, \{z\})$ as a factor common to all terms. We calculate $\sum (-)^{\#(i_k=0)} Z_{[j_1, \dots, j_L], [i_1, \dots, i_m]}(\{x^{(1)}\} | \{y\}, \{x^{(2)}\})$ in the next subsection.

8.13. **Calculation of** $\sum(-)^{\#\{i_k=0\}} Z_{[j_1, \dots, j_L], [i_1, \dots, i_m]}(\{x^{(1)}\}|\{y\}, \{x^{(2)}\})$. We write

$$(44) \quad \sum(-)^{\#\{i_k=0\}} Z_{[j_1, \dots, j_L], [i_1, \dots, i_m]} \left(\{x^{(1)}\} \middle| \{y\}, \{x^{(2)}\} \right) = \\ \frac{1}{\ell!} \lim_{\{b^{(1)}\} \rightarrow \{\infty\}} \left(b_\ell^{(1)} \dots b_1^{(1)} S \left(\{x^{(1)}\}, \{b^{(1)}\} \middle| \{y\}, \{x^{(2)}\} \right) \right)$$

where the right hand side of (44) is the degeneration of an A_1 -type scalar product. Full details are given in Appendix A, where the right hand side is expressed in determinant form.

8.14. **Factorization of** $S(\{x^{(2)}\}, \{x^{(1)}\}, \{\infty\}, \{b^{(2)}\}|\{y\}, \{z\})$. Combining the results of (43) and (44), we see that (42) can be evaluated as

$$(45) \quad S \left(\{x^{(2)}\}, \{x^{(1)}\}, \{\infty\}, \{b^{(2)}\} \middle| \{y\}, \{z\} \right) = \\ S \left(\{x^{(2)}\}, \{b^{(2)}\} \middle| \emptyset, \{z\} \right) \frac{1}{\ell!} \lim_{\{b^{(1)}\} \rightarrow \{\infty\}} \left(b_\ell^{(1)} \dots b_1^{(1)} S \left(\{x^{(1)}\}, \{b^{(1)}\} \middle| \{y\}, \{x^{(2)}\} \right) \right)$$

where both factors are A_1 scalar products, or a degeneration thereof. Due to the Bethe equations in the $\{b^{(1)}\} \rightarrow \{\infty\}$ regime (33), the first factor can be evaluated as a Slavnov determinant, that is \mathcal{S}_1 . The second factor is also a determinant, given by equation (53) in Appendix A. Using these results, we obtain

$$(46) \quad S \left(\{x^{(2)}\}, \{x^{(1)}\}, \{\infty\}, \{b^{(2)}\} \middle| \{y\}, \{z\} \right) = \Delta^{-1} \{x^{(2)}\} \Delta^{-1} \{-b^{(2)}\} \Delta^{-1} \{x^{(1)}\} \\ \times \det \left(\frac{1}{b_j^{(2)} - x_i^{(2)}} \left(\prod_{k \neq j}^m (b_k^{(2)} - x_i^{(2)} + 1) - \prod_{k \neq j}^m (b_k^{(2)} - x_i^{(2)} - 1) \prod_{k=1}^M \left(\frac{x_i^{(2)} - z_k - 1}{x_i^{(2)} - z_k} \right) \right) \right)_{1 \leq i, j \leq m} \\ \times \det \left((x_i^{(1)})^{j-1} \prod_{k=1}^L \left(\frac{x_i^{(1)} - y_k + 1}{x_i^{(1)} - y_k} \right) - (x_i^{(1)} + 1)^{j-1} \prod_{k=1}^m \left(\frac{x_i^{(1)} - x_k^{(2)} - 1}{x_i^{(1)} - x_k^{(2)}} \right) \right)_{1 \leq i, j \leq \ell}$$

This formula is the A_2 vertex-model version of equation (110) in [2].

9. COMMENTS

Because we expect SYM_4 to be integrable [13, 14], we expect to be able to compute 3-point functions, including those that involve SYM_4 local composite operators with more symmetry than A_1 , in a tractable form. But computing these 3-point functions involves off-shell/on-shell scalar products that cannot (to the best of our knowledge) be expressed in determinant form, or any other tractable form, when operators with more symmetry than A_1 are involved.

The results of [1, 2] show that there are special cases of the A_2 and higher rank off-shell/on-shell scalar products that can be computed in terms of partition functions of A_1 vertex model configurations that can be expressed as determinants.

The point of this paper is to understand the results of [1, 2] in combinatorial, vertex model terms, and more importantly to characterize the A_2 and higher rank vertex model configurations that are rank or colour independent and can be computed in A_1 terms. Aside from potential relevance to integrable statistical mechanical models, we expect our results to help in evaluating special cases of 3-point functions that involve A_2 operators such as those classified and discussed in [33].

ACKNOWLEDGEMENTS

This work was supported by the Australian Research Council, Australia, and the Centre National de la Recherche Scientifique, France. Both authors wish to thank the Institut Henri Poincaré for excellent hospitality while part of this work was done.

APPENDIX A. PARTIAL DOMAIN WALL PARTITION FUNCTIONS

A.1. Partial domain wall partition functions as limiting cases of scalar products.

The ‘partial domain wall partition functions’ $Z(\{x\}_N|\{y\}_L)$ are partition functions of A_1 -vertex model configurations of the form shown in Figure 25. More precisely, they are partition functions on $N \times L$ A_1 lattice configurations, $N \leq L$, whose top boundary is summed over the colours $\{0, 1\}$, while the state variables at the remaining boundaries are fixed as shown. A partial domain wall partition function can be viewed as **1**. A degenerate case of a domain wall partition function $Z(\{x\}_L|\{y\}_L)$, by sending $x_L, \dots, x_{N+1} \rightarrow \infty$, as in [23], or **2**. A degenerate case of a scalar product $S(\{x\}_N, \{b\}_N|\{y\}_L)$, by sending $b_N, \dots, b_1 \rightarrow \infty$, as in [21, 22, 23]. In this work we are interested in the latter interpretation.

To obtain an explicit formula for $Z(\{x\}_N|\{y\}_L)$ one can start from any expression for the A_1 scalar product $S(\{x\}_N, \{b\}_N|\{y\}_L)$, such as Slavnov’s determinant (15), which assumes the Bethe equations for $\{b\}_N$, or from the sum expression due to Izergin and Korepin [3], which does not. The final results are necessarily equivalent, since both expressions are valid in the regime $b_N, \dots, b_1 \rightarrow \infty$. Here we shall make use of the sum form, which is given by

$$(47) \quad S \left(\{x\}_N, \{b\}_N \middle| \{y\}_L \right) =$$

$$\sum_{\substack{\{x\}=\{x_I\} \cup \{x_{II}\} \\ \{b\}=\{b_I\} \cup \{b_{II}\}}} \prod_{b_I} \prod_{k=1}^L \left(\frac{b_I - y_k + 1}{b_I - y_k} \right) \prod_{x_{II}} \prod_{k=1}^L \left(\frac{x_{II} - y_k + 1}{x_{II} - y_k} \right)$$

$$\times \prod_{x_I, x_{II}} \left(\frac{x_I - x_{II} + 1}{x_I - x_{II}} \right) \prod_{b_I, b_{II}} \left(\frac{b_{II} - b_I + 1}{b_{II} - b_I} \right) Z \left(\{b_{II}\} \middle| \{x_{II}\} \right) Z \left(\{x_I\} \middle| \{b_I\} \right)$$

where we continue to define $S(\{x\}_N, \{b\}_N|\{y\}_L)$ as the partition function of Figure 6, but in the normalization in which all b weights are equal to 1. $Z(\{b_{II}\}|\{x_{II}\})$ and $Z(\{x_I\}|\{b_I\})$ are domain wall partition functions, as given by Figure 3, again in the normalization with all b weights equal to 1. From this, one can readily compute the leading behaviour as $b_N, \dots, b_1 \rightarrow \infty$. The result of the calculation is

$$(48) \quad \frac{1}{N!} \lim_{\{b\} \rightarrow \{\infty\}} \left(b_N \dots b_1 S \left(\{x\}_N, \{b\}_N \middle| \{y\}_L \right) \right) =$$

$$\sum_{\{x\}=\{x_I\} \cup \{x_{II}\}} (-)^{|\{x_I\}|} \prod_{x_{II}} \prod_{k=1}^L \left(\frac{x_{II} - y_k + 1}{x_{II} - y_k} \right) \prod_{x_I, x_{II}} \left(\frac{x_I - x_{II} + 1}{x_I - x_{II}} \right)$$

The preceding sum can be recognized as the Laplace expansion of the determinant of a sum of two matrices. Therefore we obtain a compact determinant expression for the partial domain wall partition function,

$$(49) \quad Z \left(\{x\}_N \middle| \{y\}_L \right) = \frac{1}{N!} \lim_{\{b\} \rightarrow \{\infty\}} \left(b_N \dots b_1 S \left(\{x\}_N, \{b\}_N \middle| \{y\}_L \right) \right)$$

$$= \Delta^{-1} \{x\}_N \det \left[x_i^{j-1} \prod_{k=1}^L \left(\frac{x_i - y_k + 1}{x_i - y_k} \right) - (x_i + 1)^{j-1} \right]_{1 \leq i, j \leq N}$$

This expression was obtained by Kostov in [21, 22], where the starting point of the calculation was Slavnov’s determinant, rather than the sum expression (47). For our purposes, the derivation from the sum form is essential, since in the following subsection we study the same limit but of scalar products which have no apparent determinant form.

A.2. Scalar products with varying quantum space representations. In Section 8 we encounter the objects (38) and (44) which resemble partial domain wall partition functions, but which arise as the limiting cases of more general A_1 scalar products. Namely, they come from scalar products in A_1 spin chains built from fundamental *and* anti-fundamental

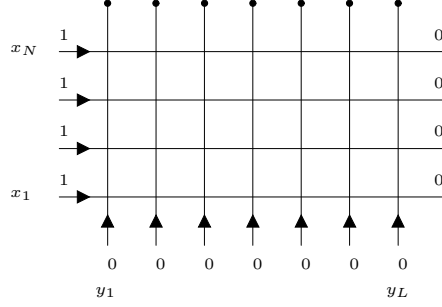


Figure 25: Lattice representation of the partial domain wall partition function $Z(\{x\}_N|\{y\}_L)$. The state variables at the top boundary are summed over the values $\{0, 1\}$.

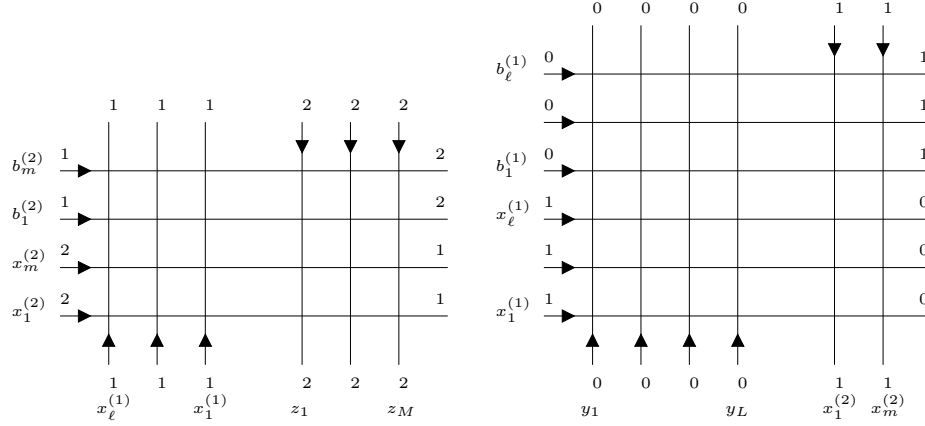


Figure 26: The scalar product $S(\{x^{(2)}\}, \{b^{(2)}\}|\{x^{(1)}\}, \{z\})$ is on the left. By taking the limit $b_m^{(2)}, \dots, b_1^{(2)} \rightarrow \infty$, it reduces to the partition function on the left of Figure 21, with summation implied over the colours $\{i_1, \dots, i_\ell\}, \{j_1, \dots, j_M\}$. On the right, the scalar product $S(\{x^{(1)}\}, \{b^{(1)}\}|\{y\}, \{x^{(2)}\})$. By taking the limit $b_\ell^{(1)}, \dots, b_1^{(1)} \rightarrow \infty$, it reduces to the partition function on the right of Figure 23, with summation implied over the colours $\{j_1, \dots, j_L\}, \{i_1, \dots, i_m\}$.

representations of the universal R -matrix, which are shown in Figure 26. In sum form ⁶ these scalar products are given by

$$(50) \quad S \left(\{x^{(2)}\}, \{b^{(2)}\} \middle| \{x^{(1)}\}, \{z\} \right) = \sum_{\substack{\{x^{(2)}\} = \{x_I^{(2)}\} \cup \{x_{II}^{(2)}\} \\ \{b^{(2)}\} = \{b_I^{(2)}\} \cup \{b_{II}^{(2)}\}}} \prod_{b_I^{(2)}} \prod_{k=1}^{\ell} \left(\frac{b_I^{(2)} - x_k^{(1)} + 1}{b_I^{(2)} - x_k^{(1)}} \right) \\ \times \prod_{b_{II}^{(2)}} \prod_{k=1}^M \left(\frac{b_{II}^{(2)} - z_k - 1}{b_{II}^{(2)} - z_k} \right) \prod_{x_{II}^{(2)}} \prod_{k=1}^{\ell} \left(\frac{x_{II}^{(2)} - x_k^{(1)} + 1}{x_{II}^{(2)} - x_k^{(1)}} \right) \prod_{x_I^{(2)}} \prod_{k=1}^M \left(\frac{x_I^{(2)} - z_k - 1}{x_I^{(2)} - z_k} \right)$$

⁶In fact we are unable to express them as determinants, because they are not candidates for the application of Slavnov's formula. This is due to the fact that either $\{x^{(1)}\}$ or $\{x^{(2)}\}$ appear as inhomogeneities in these scalar products, whereas these variables make no appearance in the Bethe equations.

$$\times \prod_{x_I^{(2)}, x_{II}^{(2)}} \left(\frac{x_I^{(2)} - x_{II}^{(2)} + 1}{x_I^{(2)} - x_{II}^{(2)}} \right) \prod_{b_I^{(2)}, b_{II}^{(2)}} \left(\frac{b_{II}^{(2)} - b_I^{(2)} + 1}{b_{II}^{(2)} - b_I^{(2)}} \right) Z \left(\{b_{II}^{(2)}\} \mid \{x_{II}^{(2)}\} \right) Z \left(\{x_I^{(2)}\} \mid \{b_I^{(2)}\} \right)$$

which is the scalar product in (38), and

$$(51) \quad S \left(\{x^{(1)}\}, \{b^{(1)}\} \mid \{y\}, \{x^{(2)}\} \right) = \sum_{\substack{\{x^{(1)}\} = \{x_I^{(1)}\} \cup \{x_{II}^{(1)}\} \\ \{b^{(1)}\} = \{b_I^{(1)}\} \cup \{b_{II}^{(1)}\}}} \prod_{b_I^{(1)}} \prod_{k=1}^L \left(\frac{b_I^{(1)} - y_k + 1}{b_I^{(1)} - y_k} \right) \\ \times \prod_{b_{II}^{(1)}} \prod_{k=1}^m \left(\frac{b_{II}^{(1)} - x_k^{(2)} - 1}{b_{II}^{(1)} - x_k^{(2)}} \right) \prod_{x_{II}^{(1)}} \prod_{k=1}^L \left(\frac{x_{II}^{(1)} - y_k + 1}{x_{II}^{(1)} - y_k} \right) \prod_{x_I^{(1)}} \prod_{k=1}^m \left(\frac{x_I^{(1)} - x_k^{(2)} - 1}{x_I^{(1)} - x_k^{(2)}} \right) \\ \times \prod_{x_I^{(1)}, x_{II}^{(1)}} \left(\frac{x_I^{(1)} - x_{II}^{(1)} + 1}{x_I^{(1)} - x_{II}^{(1)}} \right) \prod_{b_I^{(1)}, b_{II}^{(1)}} \left(\frac{b_{II}^{(1)} - b_I^{(1)} + 1}{b_{II}^{(1)} - b_I^{(1)}} \right) Z \left(\{b_{II}^{(1)}\} \mid \{x_{II}^{(1)}\} \right) Z \left(\{x_I^{(1)}\} \mid \{b_I^{(1)}\} \right)$$

which is the scalar product in (44). Using these formulae, and proceeding in analogy with the calculation in Appendix A.1, we find that

$$(52) \quad \frac{1}{m!} \lim_{\{b^{(2)}\} \rightarrow \{\infty\}} \left(b_m^{(2)} \dots b_1^{(2)} S \left(\{x^{(2)}\}, \{b^{(2)}\} \mid \{x^{(1)}\}, \{z\} \right) \right) = \Delta^{-1} \{x^{(2)}\} \\ \times \det \left[(x_i^{(2)})^{j-1} \prod_{k=1}^{\ell} \left(\frac{x_i^{(2)} - x_k^{(1)} + 1}{x_i^{(2)} - x_k^{(1)}} \right) - (x_i^{(2)} + 1)^{j-1} \prod_{k=1}^M \left(\frac{x_i^{(2)} - z_k - 1}{x_i^{(2)} - z_k} \right) \right]_{1 \leq i, j \leq m}$$

which gives rise to the second determinant in (40), and

$$(53) \quad \frac{1}{\ell!} \lim_{\{b^{(1)}\} \rightarrow \{\infty\}} \left(b_\ell^{(1)} \dots b_1^{(1)} S \left(\{x^{(1)}\}, \{b^{(1)}\} \mid \{y\}, \{x^{(2)}\} \right) \right) = \Delta^{-1} \{x^{(1)}\} \\ \times \det \left[(x_i^{(1)})^{j-1} \prod_{k=1}^L \left(\frac{x_i^{(1)} - y_k + 1}{x_i^{(1)} - y_k} \right) - (x_i^{(1)} + 1)^{j-1} \prod_{k=1}^m \left(\frac{x_i^{(1)} - x_k^{(2)} - 1}{x_i^{(1)} - x_k^{(2)}} \right) \right]_{1 \leq i, j \leq \ell}$$

which gives rise to the second determinant in (46).

REFERENCES

- [1] J Caetano and P Vieira, private communication, March 2012.
- [2] M Wheeler, *Scalar products in generalized models with $SU(3)$ -symmetry*, [arXiv:1204.2089](#)
- [3] V E Korepin, N M Bogoliubov, A G Izergin, *Quantum inverse scattering method and correlation functions*, Cambridge University Press (1993)
- [4] F H L Essler, H Frahm, F Gohmann, A Klumper, V E Korepin, *One-dimensional Hubbard model*, Cambridge University Press (2005)
- [5] R J Baxter, *Exactly solved models in statistical mechanics*, Dover (2008)
- [6] V E Korepin, *Calculation of norms of Bethe wave functions*, Commun. Math. Phys. **86** (1982) 391–418
- [7] N Yu Reshetikhin, *Calculation of the norm of Bethe vectors in models with $SU(3)$ -symmetry*, Zap. Nauchn. Sem. **150** (1986) 196–213
- [8] N A Slavnov, *Calculation of scalar products of wave functions and form factors in the framework of the algebraic Bethe Ansatz*, Theor Math Phys **79** (1989) 502–508
- [9] I Kostov and Y Matsuo, *Inner products of Bethe states as partial domain wall partition functions*, [arXiv:1207.2562](#)
- [10] O Foda and M Wheeler, *Variations on Slavnov's scalar product*, JHEP **10** (2012) 096, [arXiv:1207.6871](#)
- [11] M Gaudin, *La fonction d'onde de Bethe*, Masson, Paris (1983)
- [12] M Gaudin, *Bose Gas in One Dimension. II. Orthogonality of the Scattering States*, J Math Phys **12** (1971) 1677–1680.
- [13] N Beisert *et al.*, *Review of AdS/CFT Integrability: An Overview*, Letters in Mathematical Physics **1** (2011) 163, [arxiv:1012.3982](#), and the reviews that it introduces.
- [14] D Serban, *Integrability and the AdS/CFT correspondence*, J Phys **A44** (2011) 124001 [arXiv:1003.4214](#)
- [15] J Escobedo, N Gromov, A Sever and P Vieira, *Tailoring three-point functions and integrability*, J of High Energy Phys **2011** (2011) Number 9, 28 [arXiv:1012.2475](#)
- [16] J Escobedo, N Gromov, A Sever and P Vieira, *Tailoring Three-Point Functions and Integrability II. Weak/strong coupling match*, J of High Energy Phys **2011** (2011) Number 9, 29 [arXiv:1104.5501](#)
- [17] N Gromov, A Sever and P Vieira, *Tailoring Three-Point Functions and Integrability III. Classical Tunneling*, J of High Energy Phys (2012) Number 7, 1–31, [arXiv:1111.2349](#)
- [18] O Foda, *$\mathcal{N} = 4$ SYM structure constants as determinants*, J of High Energy Phys **2012** (2012) Number 3, 96 [arXiv:1111.4663](#)
- [19] O Foda and M Wheeler, *Slavnov determinants, Yang-Mills structure constants, and discrete KP, in Symmetries, Integrable Systems and Representations*, K Iohara, S Morier-Genoud and B Rémy, Editors, Springer Proceedings in Mathematics and Statistics, Springer, 2012 [arXiv:1203.5621](#)
- [20] C Ahn, O Foda and R I Nepomechie, *OPE in planar QCD from integrability*, J of High Energy Phys (2102) Number 6, 1–25 [arXiv:1202.6553](#)
- [21] I Kostov, *Classical Limit of the Three-Point Function from Integrability*, [arXiv:1203.6180](#)
- [22] I Kostov, *Three-point function of semiclassical states at weak coupling*, [arXiv:1205.4412](#)
- [23] O Foda, M Wheeler, *Partial domain wall partition functions*, J of High Energy Phys (2012) Number 7, 186 [arXiv:1205.4400](#)
- [24] N Gromov and P Vieira, *Quantum integrability for three-point functions*, [arXiv:1202.4103](#)
- [25] D Serban, *A note on the eigenvectors of long-range spin chains and their scalar products*, [arXiv:1203.5842](#)
- [26] S Belliard, S Pakuliak, E Ragoucy, N A Slavnov, *Highest coefficient of scalar products in $SU(3)$ -invariant integrable models* J Stat Mech (2012) P09003, [arXiv:1206.4931](#)
- [27] S Belliard, S Pakuliak, E Ragoucy, N A Slavnov, *The algebraic Bethe ansatz for scalar products in $SU(3)$ -invariant integrable models*, J Stat Mech (2012) P10017, [arXiv:1207.0956](#)
- [28] A G Izergin, *Partition function of the six-vertex model in a finite volume*, Sov Phys Dokl **32** (1987), 878–879
- [29] N Kitanine, J M Maillet, and V Terras, *Form factors of the XXZ Heisenberg spin-1/2 finite chain*, Nucl Phys B **554** [FS] (1999) 647–678, [arXiv:math-ph/9807020](#)
- [30] M Wheeler, *An Izergin–Korepin procedure for calculating scalar products in six-vertex models*, Nucl Phys **B852** (2011) 468–507, [arXiv:1104.2113](#)
- [31] S Belliard, S Pakuliak, E Ragoucy, N A Slavnov, *Bethe vectors of $SU(3)$ -invariant integrable models*, [arXiv:1210.0768](#)
- [32] S Belliard, S Pakuliak, E Ragoucy, N A Slavnov, *Form factors in $SU(3)$ -invariant integrable models*, [arXiv:1211.3968](#)
- [33] O Foda, Y Jiang, I Kostov and D Serban, *A tree-level 3-point function in the $su(3)$ -sector of planar $\mathcal{N} = 4$ SYM*, to appear.

¹ DEPT OF MATHEMATICS AND STATISTICS, UNIVERSITY OF MELBOURNE, PARKVILLE, VIC 3010, AUSTRALIA
² LABORATOIRE DE PHYSIQUE THÉORIQUE ET HAUTES ENERGIES, CNRS UMR 7589 AND UNIVERSITÉ PIERRE ET MARIE CURIE - PARIS 6, 4 PLACE JUSSIEU, 75252 PARIS CEDEX 05, FRANCE
E-mail address: omar.foda@unimelb.edu.au, mwheeler@lpthe.jussieu.fr